Response to Anonymous Referee #1 comments

Overall, the manuscript presents a thorough analysis of four biomass burning events monitored in Finokalia station. Plumes are measured by their particle numbers, sizes, chemistry, CCN activity and hygroscopicity, making it possible to assess the climatic impacts of these biomass burning (BB) aerosols. However, the manuscript does not give any quantitative information about these BB events impact for climate, rather it satisfies with reassuring the previous observations on the organics aerosols impacts on aerosol hygroscopicity. As such, its originality is not very high, yet in Introduction the authors promise "The originality of this study relies on the fact that… very view studies focus on hygroscopicity of ambient biomass burning aerosol for a range of atmospheric aging, which is addressed here". This indeed is very interesting and I find the manuscript well written and important, yet I would hope to see slightly deeper analysis of the background conditions for each of the events, to give the manuscript the originality it deserves. Below are my detailed suggestions which I hope the authors would address before manuscript publication in ACP.

Response: *We thank the reviewer for the well-articulated and thoughtful arguments. Our analysis was approached in view of these concerns to include more information about the fire events, which will help with the aspects of aging and atmospheric processing of the plumes. We have further elaborated on these points in the revision for clarity. In order to strengthen the aspect of the direct impact of biomass burning, we have included a section on calculations of potential droplet number in marine boundary layer clouds formed over Finokalia. The focus of the analysis is on the relative impact of BBOA CCN on CDNC, supersaturation and the contributions of aerosol number and hygroscopicity on the resulting CDNC. Below is our response to the comments raised in italics.*

General comments:

1) Aging of the BB plumes is mentioned many times, and terminology such as "aged" or "freshly-emitted" BB aerosol are used. Yet, it's not very clear what are the criteria for more or less aged, or fresh, plumes? Also no information on transport conditions (how many hours air masses traveled, on what time of day and over which route) is given, nor any information on the type of fires (grass, forest, soil type). As current, it seems the age of each plume is rather deduced based on measured aerosol quantities, even if vice versa, the BB plume age should be predetermined. Could the authors clearly state how the age of each plume and BB aerosol was determined, and analyse the impact of this aging on each of the remaining measured quantities (as promised in introduction)?

Response: *All the information concerning the fire events are given in detail in the publication of Bougiatioti et al. (2014) (ACP). In this publication we wanted to focus on the hygroscopicity and the CCN during these events. Nevertheless, we will try including some more information on the issues raised by the anonymous referee in the revised version of the manuscript.*

See page 24, lines 1076-1082 of the current file

2) In many occasions the manuscript analysis the "change" of observed aerosol quantities caused by BB emissions (e.g. 21551 lines 1-2 and 12-15 and 21-23; 21552 lines 1-2; 21555 lines 5-6; etc.). However, it's not always very clear what is the reference point? Measured values prior to BB events, in the beginning of the events, or something else? Could this be more clearly stated? Also, is the reference point relevant for the current location, or representing e.g typical conditions at Finokalia? Do the air masses remain unchanged over the course of each of the events or may these play a role in observed changes?

Response: *Good point. As a reference point, the averaged data from at least 6 hours of data prior to the arrival of the plume time are taken. This will be clarified in the revised text. Prior to the events, conditions are regarded as characteristic for a background site as Finokalia.*

See page 26, lines 1141-1143 of the current file

Minor comments:

p. 21552 lines 1-2: Authors state that CCN concentrations increase during the majority of the BB events. I find it very surprising if during a BB event, CCN concentrations are not increasing? Was the site affected by some other aerosol sources on those times when concentrations did not increase (compared to reference)?

Response: *The increase of the CCN concentrations during the BB events was more pronounced, depending on the proximity of the fire and therefore, the travel time of the air masses. The only case when concentrations did not increase considerably was the event from Croatia, when air masses had a travel time of around 16h before reaching the station. Probably air masses were more diluted therefore the effect the biomass burning event had on CCN concentrations was less intense. This will be clarified in the revised text.*

See page 26, lines 1139-1157 of the current file

p. 21553 line 24-25; 21557 lines 1-2 and lines 18-19: Slightly confusing and mixed information is given on observed particle internal/external mixing states. Could the authors check that all this information is consistent?

Response: *We would like to thank the reviewer for pointing out this inconsistency. Indeed, for the HTDMA the majority of the data exhibited unimodal distributions, apart from the data during the arrival of the smoke plumes. The confusing sentence that bimodal distributions were not taken into account for this specific study is referring to the comparison between kappa values derived from both the CFSTGC and the HTDMA, which will be clarified in the text. Also the statement that "all selected particle fractions were internally mixed" is modified according to the rest of the findings in the manuscript.*

See page 31, lines 1397-1403 of the current file

p. 21555 line 25: Authors say that aging of smaller particles takes longer than aging of larger particles. Maybe so, but in this case, how they rule out e.g. a possibility that these smallest particles were not just born later by a secondary route, but are actually from the same source?

Response: *Good point. We do not rule out the possibility that the smallest particles were not formed later by a secondary route, it is a suggestion that the aging of smaller particles takes longer than aging of larger particles. Indeed, because of the difference in mass and interface with the gas phase, larger particles would age later than smaller ones. The text has been modified accordingly.*

See pages 30-31, lines 1353-1368 of the current file

p. 21563 lines 8-9: Importance of coagulation vs. condensation could also be calculated by a dynamical model, having all this information the authors have. Would this support the statement that for 60 nm particles coagulation is dominant over condensation?

Response: *We do agree that the discussion on the importance of coagulation vs. condensation needs strengthening and this is why the variance of the chemical composition of each particle*

size is now included in the revised version of the manuscript. According to Jacobson (2002) and numerical simulations, coagulation internally mixes a greater fraction of larger particles than smaller particles, and condensation increases the fractional coating of small particles more than it does large particles. The route of secondary formation of the smaller particles during the transport of the smoke is now also added in the text.

See pages 30-31, lines 1353-1368 of the current file

p. 21561 lines 1-2: Is kappa(BBOA) factor from ACSM seen to coincide with the occurrence of less-hygroscopic mode seen in HTDMA?

Response: *In general, the occurrence of two modes of different hygroscopicity seen by the HTDMA was not very frequent, but all of them occurred during the arrival of the smoke and indeed the derived* $kappa_{BBOA}$ *is very close to the kappa of the less hygroscopic mode seen by the HTDMA.*

See page 35, lines 1541-1544 of the current file

Typo: 2nd sentence of summary has repetition.

Response: *Done, the repeated sentence is deleted.*

Jacobson, M.Z.: Analysis of aerosol interactions with numerical techniques for solving coagulation, nucleation, condensation, dissolution, and reversible chemistry among multiple size distributions, J. Geophys. Res.: Atmospheres,107, D19, 4366, doi:10.1029/2001JD002044, 2002.

Response to Anonymous Referee #2 comments

The paper by A. Bougiatioti is presenting a study on the hygroscopicity and CCN properties changes of aerosols when biomass burning (BB) events are transported to the Finokalia site. The study is focused on a two or three months period (which is not very clear) when four BB events occurred. Although the retrieval of the hygroscopic properties of BB aerosols would be interesting to the scientific community, there are many (major) points that have to be clarified before the manuscript is considered for publication:
(1) there is a need to better describe the statistical analyses used. A careful statistical analysis of the aerosol properties when they are not affected by BB (including their variability over the period chosen) compared to the change in these properties when the plume is sampled at the site (the choice of the boundary of the plume is important: how is this performed? Is it based on the BBOA derived from the PMF, or BC? Is there a threshold used and on which parameter?) is needed. Then, within the plume, the methodology for separating the fraction of aerosols, which are originating from the BB event and their properties from ambient aerosols that have mixed along the transport path is not very clear. Can the external mixing information from the HTDMA data and the PMF analysis be combined to compute an increase of CN and CCN number concentrations due to the contribution of BB aerosols? Can this be compared to the increase of CCN number computed with the first approach (comparison of outside vs inside the plume)? Which multivariable regression analysis is used to retrieve the different organic fraction hygroscopicity parameter? What are the uncertainties?

***Response**: We thank the anonymous referee for the thoughtful review. Most of the issues raised were also concerns of the other anonymous referees therefore we have further elaborated on these points in the revision manuscript. Nevertheless, all the details concerning the identification and source apportionment of the organic aerosol are provided in the separate publication of Bougiatioti et al. (2014). On the other hand, more details concerning the multivariable regression analysis to retrieve the hygroscopicity parameter of each fraction will be provided in the revised version of the manuscript.*

See page 34, lines 1521-1523 and 1536-1538 of the current file

(2) There are inconsistencies in the data set. Even though average kappa's derived from HTDMA and CCN measurements agree within 30% over the whole period (Table 2), a simple reading of Fig6 and Fig7 shows that the discrepancy can be much higher over smaller periods. This needs to be better commented.

***Response**: Indeed overall kappas derived from the HTDMA and CCN agree within 30%. Differences larger than 30% in kappa values derived by the CCNC or the HTDMA are probably caused by the following reasons:*
1) HTDMA detects all sampled particles including the hydrophobic ones (i.e. GF=1; κ=0). On the other hand CCNC will detect only activated particles. In cases of coexisting hygroscopic and hydrophobic, externally mixed, populations $\overline{\kappa_{HTDMA}}$ *(i.e., the average kappa value which is representative of the hygrsocopic properties of the entire sampled particle population) accounts for both (c.f. equation 6 in the manuscript), while only activated particles are accounted in the determination of κCCN.*
2) The hygroscopic parameter of the organic fraction may differ in sub- and super-saturated conditions (e.g. Henning et al., 2012; Chan, M. N., & Chan, C. K, 2007; Wex et al., 2009; Dusek et al, 2011).
Another possibility is that the particles originated from biomass burning may, among others, include surfactants, which influence the discrepancies between the κ-HTDMA and κ-CFSTGC

values.
Furthermore,water adsorption on nealry hydrophobic particles will be more pronounced at super-than in sub- saturated conditions. In the case of the larger sampled particles, this may lead to their activation and detection by the CCNC, thus increasing the difference between κCCN and $\overline{\kappa_{HTDMA}}$ *deruved values.*

See page 32, lines 1409-1422 and lines 1438-1442 of the current file

(3) The global impact of the results is not very clear:
a. the impact on atmospheric chemistry of the water contained in the organic fraction of the aerosol should be better evaluated: what is the increase of LWC due to organic BB aerosols compared to the LWC that the whole aerosol population would contain (actually, only the contribution of BB organic aerosols relative to the total organic content is evaluated)? Would this increase in LWC really favour chemical reactions that would not have taken place?

Response*: The role and impact of LWC is the focus of a different publication on its own (Nikolaou et al., 2015, ACPD) but the contribution of biomass burning aerosol to the total organic water of the aerosol is mentioned due to the possible atmospheric implications.*

See Section 3.8 page 35 of the current file for the droplet calculations

b. The same is true for the direct impact: what is the contribution of BB aerosol liquid content compared to the rest of the population?

Response*: In order to strengthen the aspect of the direct impact of biomass burning, we have included a section on calculations of potential droplet number in marine boundary layer clouds formed over Finokalia. The focus of the analysis is on the relative impact of BBOA CCN on CDNC, supersaturation and the contributions of aerosol number and hygroscopicity on the resulting CDNC. Overall, it seems that there are differences in the droplet number concentrations, impacted by both the distance and from the intensity of the events. The higher the proximity, the lowest the contribution of the chemistry (kappa) to the droplet formation. As the distance grows higher, the concentrations get lower due to dilution, and the influence of the chemical composition gets higher.*

See Section 3.8 page 35 of the current file for the droplet calculations

c. The impact on the total number of CCN is not clear neither, as the paper is showing changes in CCN number at variable sursaturations. What is the increase of CCN number due to BB at a given sursaturation?

Response*: For all the fire events, CCN concentrations are provided at the point of critical flow, corresponding to a critical supersaturation, as explained in detail in the Methodology section. Within each fire event, critical supersaturation for e.g. 120 nm particles was 0.14±.0.03 for the Euboea event, or for the 100 nm particles was 0.19±0.03 for the same event. Therefore it is expected that the differences in CCN concentration number are caused by the presence of the BB plume, rather than the different supersaturation.*

See page 26, lines 1156-1161 of the current file

Detailed comments are given below:

Page 21542, lines 23-25 : "Laboratory and field studies suggest that the water-soluble component of biomass burning aerosol is highly hygroscopic, about half of ammonium sulfate".

Not clear what half of ammonium sulfate is related to. Is half of BB aerosol ammonium sulfate ? to reformulate

***Response**: Indeed, the "about half of ammonium sulfate" refers to the hygroscopicity parameter kappa, the text now reads "…is highly hygroscopic, with a hygroscopicity parameter about half of that of ammonium sulfate".*

See page 18, lines 812-814 of the current file

Page 21549, line 23, I suppose the authors mean 18 august 2012 and not 1992

***Response**: Indeed. Amended.*

figure 2c : Caliop shows that the smoke is travelling at higher latitude than the finokalia station right ? does this imply that the contribution of BB aerosol to the global mass loading is underestimated from the ground-based in situ measurements?

***Response**: The Caliop overpass over Crete, on 19 August 2012 between 00:27–00:40 and 11:34–11:47 UTC, is NW of the Finokalia station (Fig. 2a). For the 00:27–00:40 UTC time slot, based on the Caliop data (Fig. 2c), we can clearly see the presence of smoke aerosols mixed with the prevailing polluted dust and marine aerosols in the first 3 km height of the lower troposphere. This implies that for this time slot, the BB aerosols sampled by the ground-based in situ measurements at Finokalia would contribute less (due to dilution) to the global aerosol mass loading than, if measured, over the Western Crete. The text has been rephrased to "According to this classification, over Western Crete the presence of polluted dust (mixed with smoke and marine aerosols) prevails within the marine boundary layer, which for Finokalia is extending up to 0.8–1.2 km height, close to the mean value of 1 km reported by Kalivitis et al. (2007). This implies that for the 00:27–00:40 UTC time slot, the BB aerosols sampled by the ground-based in situ measurements at Finokalia would contribute less (due to dilution) to the global aerosol mass loading than, if measured, over the Western Crete."*

See page 25, lines 1116-1118 of the current file

Page 21550, line 23 could you recall what is "the whole measurement period"? it is not clear.

***Response**: Amended.*

See page 25, lines 1121-1122 of the current file

Figure 3 : need more dates on the x axis

***Response**: Amended.*

See page 51 of the current file

Page 21551, lines 1-2 : "the contribution of organics and BC increased substantially (from 34.9 to 46.5% for organics and from 6.1 to 9.5% for BC) with a simultaneous reduction of that of sulfate" To which period is the increase of BC and organics relative to ? Are those really substantial increases? What is the natural variability in organic and BC concentrations outside the BB events? Are percentages really relevant ? (BC contribution would increase if other components decrease, even if it stays constant.. ?) maybe absolute concentrations would be useful as well here?

***Response**: This increase refers to the observed average concentrations during all fire events, compared to the rest of the timeseries. The percentages express the relative contribution of each component to the total mass during these fire events. These increases are verified to be caused by the presence of BB plumes as described in detail in Bougiatioti et al. (2014), both as far as organics but also as BC is concerned, via source apportionment analysis. Especially for BC, during all BB events there is a clear increase from the contribution of wood burning, compared to that of fossil fuel.*

See page 25, lines 1129-1133 of the current file

Page 21551, line 12 can you precise which size range is considered as "larger particles"?

***Response**: Amended. It refers to particles with diameter larger than 100 nm.*

See page 26, lines 1149-1152 of the current file

Page 21551, line 13-14 "concentrations exhibited an increase that for the case of the Chios fire was around 65 %, for the Croatia fire around 50 %, the Euboea fire 88% and the Andros fire around 150 %." How was this determined? An increase relative to what ? to the mean concentration over the larger period of measurement (from April to September) ? average concentration during all BB events compared to the average concentration shown figure 3 (20 august to 18 sept) ?

***Response**: The text refers to CCN concentrations higher than the ones before the arrival of the smoke plume (average of around 6 hours). This will be clarified in the text.*

See page 25, lines 1147-1149 of the current file

Figure 4 : not easy to read : small and all lines are surimposed

***Response**: The complexity of this figure with all the information that is included limits somewhat the resolution of this figure. Nevertheless the readability is improved once the four figures are placed in one column instead of two.*

See pages 52-53 of the current file

Page 21552, line 1-3 : "The data shown in Fig. 4 indicates that during the majority of the identified biomass burning events, CCN concentrations for the larger particles sizes increase, tracking the BBOA trend." this is not really the case for the Croatia fire event.
I am not sure that you can really compare CCN number concentration for different sizes, since they are given for different sursaturations? Larger particles CCN concentrations might increase but if you need higher sursaturations for activating them, they might not contribute to the relevant CCN number concentration if the needed supersaturations needed to activate them are not realistic. In my opinion, increases in CCN numbers should be evaluated at a given supersaturation. If the goal of this discussion is to show that 100 nm particles concentrations are increased in the smoke plume, than it is easier to simply evaluate the increase of this size range from the SMPS size distribution?

***Response**: As mentioned in p.25551, lines 18-20, CCN concentrations are given at the point of critical activation flow Q_{50}, corresponding to the instantaneous supersaturation for each particle size. During the separate events, the derived critical supersaturations for a given particle size did not vary by more than 13.6%, being less for the smaller particle sizes. This information can be included in the revised text. The goal of the discussion is to show that smoke plumes contain larger more CCN-active particles, not just more particles.*

See page 26, lines 1161-1163 of the current file

Page 21552, line 8 : two times “that”

***Response**: Done.*

Page 21552, lines 12_16 : “It appears that when the BB event is combined with a NPF event within a few hours, 60nm particles are strongly influenced and their CCN concentrations increase considerably. A detailed discussion on these events and their contribution to CCN concentrations is provided by Kalivitis et al. (2015).” Could you shortly give the conclusions from the Kalivitis paper ? Is NPF unambiguously associated to BB event (favoured by BB events) ? If NPF is occurring anyway (independatly of the presence of a BB plume), it should be mentioned otherwise the reader is mislead into the idea that the 60 nm CCN concentration increase is due to the presence of the BB plume.

***Response**: This is a good point. The goal was not to suggest that the 60 nm CCN concentration occurs from the BB plume, rather than to explain that the increase coincides with a NPF event. The exact mechanism for NPF is not known, therefore it is not unambiguously favored by BB events. If that were true, all events would be followed by NPF, which is not the case. It is merely the combination of the two we wanted to point out.*

See page 27, lines 1184-1204 of the current file

Page 21552, lines 25-28 : “First of all, it can be seen that apart from the 60nm particles, the remaining sizes appear to be unaffected by the presence of smoke, as their activation fractions at supersaturation levels as low as 0.4% remain, more or less, stable and very close to unity throughout the events.” Are the CCN concentrations again a function of supersaturation or are they given for a given supersaturation? there are no indication of the supersaturation on figure 5, to relate to the comments mentioning them in the text.

***Response**: The activation fractions are derived from the asymptote of the fitting to a sigmoidal function of the CCN/CN ratio during each supersaturation cycle and is therefore representative for high supersaturations (ss>0.6%). This is the case for all data, for all particle sizes. This will be clarified in the revised text.*

See page 27, lines 1220-1222 of the current file

Page 21554, lines 10-12 : “Most of the accumulation mode particles result from condensation of secondary sulfates, nitrates and organics from the gas phase and coagulation of smaller particles (Seinfeld and Pandis, 2006)” Accumulation mode particles can also originate from primary emission processes (combustion, but also marine aerosols have a large contribution (by number) in the accumulation mode) those can contribute to the particles hygroscopicity while not being measured by the ACSM.

***Response**: Good point. In order to examine contribution by constituents not measured by the ACSM to the accumulation mode particles we compared the mass derived from the ACSM+BC and the integrated volume distribution from the SMPS converted to mass. During the examined fire events, the ACSM-BC was on average 68.6±19.3% of the SMPS-derived mass. Therefore this is an indication that indeed, part of the accumulation mode particles that may contribute to the particles’ hygroscopicity during these events, are not being measured by the ACSM. The text will be changed accordingly to include this difference in mass and the different origin of accumulation mode particles that may contribute to the particles’ hygroscopicity.*

See page 29, lines 1297-1303 of the current file

Page 21555, lines 21-25 : "It is immediately apparent that the chemical dispersion is reduced with increasing particle size. 60nm particles exhibit the highest dispersion and especially the ones from the Chios fire, suggesting that the smaller particles retain their characteristics for a longer period and their aging takes longer that for the larger particles." There is no indication earlier in the manuscript that 60 nm particles are actually originating from BB emissions. There is no size segregated chemical analysis to show this. Would there be other indication that they are?

***Response**: Based on the derived kappa values for each particle size and the chemical composition from the ACSM, the volume fractions for organics and inorganics (mainly ammonium sulfate) were estimated for each particle size. It occurs that 60 nm particles are, on average, 89% composed of organics (the respective values for 80, 100 and 120 nm particles are 70, 50 and 41%). As the main constituent during those events is the biomass burning (both BBOA and OOA_BB) then most probably the 60 nm particles are indeed originating from BB emissions. This information will be added in the revised manuscript.*

See page 29, lines 1289-1294 of the current file

Page 21555, lines 14-27 : isn't it possible that the dispersion on kappa value also reflects the mixing with other aerosol types than the BB ones and not only processing of the BB aerosol ? The BB plume does not contain only processed (or fresh) BB but other pollution/natural aerosol. The history of the air mass before arrival to the sampling site is mainly determining how the BB is diluted into other aerosol types.

***Response**: Based on the aforementioned comment, the chemical dispersion of kappa values within the 60 and 80 nm particles, which are mostly composed of organics, is mostly due to the processing of the BB aerosol. For the larger particles, indeed, chemical dispersion may be also due to mixing with other types of aerosol. It all depends on which type of aerosol prevails in the volume fractions and interacts, thus, with the other types of aerosol. This will be added along with the estimate of the composition of each particle size.*

See page 30, lines 1356-1372 of the current file

Page 21556, lines 1-4 : "This behaviour of the small particles… coagulation mostly occurs for smaller particles and increases the external mixing of those particles by bringing together particles of different nature." I don't see the link between this sentence and the previous one. Which behavior of the small particles are the authors referring to? Coagulation creates internal mixing, external mixing is when the different chemical components are on different particles of the same size. The whole paragraph (until line 25) is confusing, and based on speculation on coagulation/condensation that ignore mixing with other particle type during transport.

***Response**: "This behavior" is referring to the increased chemical dispersion that the 60 nm particles exhibit. The sentence will be changed accordingly for clarification in the revised text. Nevertheless, all reviewers have raised the same issue on the interpretation of the results based on coagulation/condensation. We do agree, that the most probable process that justifies the obtained results is the formation of the smaller particles during the transit by secondary aerosol formation from condensation of mostly organic components (which is seen by the large mass fraction of organics in the smaller particles sizes, as already mentioned). We would like to thank all the reviewers for the scientific quality amelioration of our study. The whole discussion we be changed accordingly in the revised text.*

See page 30, lines 1356-1372 of the current file

Page 21556, lines 26-27: "During the focus period…" Do you mean outside BB events?

***Response**: The sentence corresponds to the time periods of the BB events as well as few days before and after the events.*

See page 31, lines 1400-1402 of the current file

Page 21557, lines 9-11 : "Given that the solution of the resulting droplets may be non-ideal, the constituents may be partially soluble and the phases may not be completely separated, it is not surprising that the HTDMA-derived kappa_HTDMA values are somewhat lower" which droplets ? Non ideality would account for more than 30% discrepancy?

***Response**: For ambient particles, a difference of 30% between kappa-CFSTGC and kappa-HTDMA are common. In the study of Wu et al. (2013) κ derived from CCN measurements was around 30% (varying with particle diameter) higher than that determined from hygroscopic growth measurements. This is attributed to the fact that both, substance individual and mixture κ values at 86% RH are often significantly lower than those for higher RHs and under supersaturated conditions (Petters and Kreidenweis, 2007). Apart from non ideality of the solution, the presence of surfactants produced during biomass burning events may also increase the discrepancies between κ-HTDMA and κ-CCN. This will also be added in the revised text. Overall, differences between κ values obtained from CCNc and HTDMA measurements are still under investigation in laboratory experiments. Pinpointing the exact reason of these discrepancies, in the current study, is rather difficult as we lack the exact chemical composition of the studied particles.*

See page 32, lines 1412-1445 of the current file

Page 21557, lines 16-18 "During the two most intense fire events where the smoke plume had the least transit and atmospheric processing time (i.e. during the Chios and Euboea fire) all sizes exhibited two different hygroscopic modes (Tables 3 and 4; Fig. S3 in the Supplement)." This feature clearly indicates that BB particles were externally mixed with particles of other origins, and that a direct link between the dispersion of kappa and ageing can not be drawn, right?

***Response**: As mentioned further on in the text, these two different hygroscopic modes can be due to the presence of freshly emitted particles and more processed ones, rather than particles of other origin. Positive Matrix Factorization analysis does not recognize any other possible factors e.g. traffic and air masses have not traveled over Greek mainland to be influenced by other major sources. Therefore there is a direct link between the ageing of particles which is reflected in the changes in kappa.*

Figure 7 (compared to figure 6) : the hygroscopicity parameters derived from the HTDMA decrease with increasing particle size (fig 7), while it was the opposite for CCN-derived kappas (fig 6). Can you comment on this ? For the 120 nm particles kappa derived from both techniques disagree by far more than the 30 % mentioned in the text and calculated as an average Table 2 (could be a factor 4 between the two differently derived kappa's!)

***Response**: This is a good point. The kappas derived from the CFSTGC are derived from the particles that are activated in the instrument. On the other hand, the HTDMA measures under sub-saturated conditions particles that are not "seen" by the CCN chamber; if some particles do not grow they are directly assigned with a growth factor equal to one (i.e. κ=0), subsequently reducing considerably the derived kappa value. 60 nm particles will activate (if they actually do activate) at higher supersaturations and be detected by the CFSTGC. On the other hand they are all counted by the HTDMA. 120 nm particles activate at lower supersaturations but*

as they are, in most of the cases, internal mixtures of more and less hygroscopic matter, their κ-HTDMA will be significantly lower.

See page 32, lines 1412-1445 of the current file

Page 21557, line 21: "These distinct modes were not observed during the rest of the events" Were not observed during the other two events?

***Response**: Amended. The text now reads "These distinct modes were not observed during the other two events, probably due to …".*

See page 32, lines 1432-1433 of the current file

Page 21557, line 29: "Adler et al. had also observed…" This does not necessarily mean that the second larger mode that you observe is entirely due to BBOA.

***Response**: We never said that the second larger mode is entirely due to BBOA, this is why we say that it is "probably freshly emitted…in combination with larger, more processed ones". For clarification we will rephrase to "which can be partially due to the presence of freshly emitted….".*

See page 32, lines 1446-1448 of the current file

Page 21560, line 26: the multivariable regression analysis should be described

***Response**: The multivariable regression analysis is performed within the excel environment. The overall observed hygroscopicity parameter is assumed to be the linear combination of the different components:*

$$\kappa_{CCN} = \varepsilon_{inorg}\kappa_{inorg} + \varepsilon_{BBOA}\kappa_{BBOA} + \varepsilon_{OOA\_BB}\kappa_{OOA\_BB} + \varepsilon_{OOA}\kappa_{OOA}$$

where κ_i are the hygroscopicity parameters of the main aerosol constituents and ε_i the respective mass fractions. At each data point during the fire events one equation is obtained thus a set of 228 equations is obtained for all the dataset. More details concerning the confidence level, the standard error for each variable and p-value will be provided in the text.

See page 34, lines 1519-1524 of the current file

Page 21561, line 13-14: Finally, it seems that the biomass burning organic aerosol becomes more hygroscopic, by almost a factor 2, with atmospheric processing" Is this conclusion derived from the comparison of the kappa_BBOA with the kappa_OOA-BB?

***Response**: This is correct. Based on our analysis κ_{BBOA}=0.057 and κ_{ooa_BB}=0.138.*

Page 21561, line 15: "Using average diurnal profiles..." Were these average performed over the 4 BB events? The figure should show the standard variation.

***Response**: Good point. The average diurnal profiles are derived for the whole measurement period. Standard deviation in the form of error bars is added to Figure 8.*

See page 57 of the current file

Page 21562, lines 7-9 : two times "for the most intense event"

***Response**: Amended.*

Page 21563, line 14-15: "…larger particles appear not to be affected as far as their CCN-activity is concerned". This contradicts p21562 line 21: "hygroscopicity decreases for all sizes"

***Response**: The first part for larger particles' CCN activity refers to the activation fractions and not to the hygroscopicity. This will be clarified in the text.*

See page 27, lines 1220-1229 of the current file

References

Chan, M. N., & Chan, C. K.: Mass transfer effects on the hygroscopic growth of ammonium sulfate particles with a water-insoluble coating. Atmos. Environ., 41(21), 4423-4433, 2007.

Dusek, U., Frank, G. P., Massling, A., Zeromskiene, K., Iinuma, Y., Schmid, O., Helas, G., Hennig, T., Wiedensohler, A., and Andreae, M. O.: Water uptake by biomass burning aerosol at sub-and supersaturated conditions: closure studies and implications for the role of organics. Atmos. Chem.Phys. 11, no. 18, 9519-9532, 2011.

Henning, S., Ziese, M., Kiselev, A., Saathoff, H., Möhler, O., Mentel, T. F., Buchholz, A., Spindler, C., Michaud, V., Monier, M., Sellegri, K., and Stratmann, F.: Hygroscopic growth and droplet activation of soot particles: uncoated, succinic or sulfuric acid coated. Atmos. Chem. Phys., 12, 4525-4537, doi:10.5194/acp-12-4525-2012, 2012.

Wex, H., Petters, M. D., Carrico, C. M., Hallbauer, E., Massling, A., McMeeking, G. R., Poulain, L., Wu, Z., Kreidenweis, S. M., Stratmann, F.: Towards closing the gap between hygroscopic growth and activation for secondary organic aerosol: Part 1 – Evidence from measurements, Atmos Chem. Phys., 9, 3987-3997, 2009.

Wu, Z.J., Poulain, L., Henning, S., Dieckmann, K., Birmili, W., Merkel, M., van Pinxteren, D., Spindler, G., Müller, K., Stratmann, F., Herrmann, H., and Wiedensohler, A.: Relating particle hygroscopicity and CCN activity to chemical composition during the HCCT-2010 field campaign, Atmos. Chem. Phys., 13, 7983-7996, 2013.

Response to Anonymous Referee #3 comments

The paper presents case studies of aerosol hygoscopicity and CCN-activity as recorded at the Finokalia measurement station in the presence of biomass burning influence from Greece or Croatia. While not revolutionary, the paper presents useful data on the hygroscopicity of ambient aerosol particles, and the analysis and discussion presented are generally reasonable. I therefore recommend publication in ACP after the following, mostly technical, comments have been addressed satisfactorily.

Response: *We thank the anonymous referee for the thoughtful review. Most of the issues raised were also concerns of the anonymous referee #2 therefore we have further elaborated on these points in the revision manuscript. Finally, in order to strengthen the aspect of the direct impact of biomass burning, we have included a section on calculations of potential droplet number in marine boundary layer clouds formed over Finokalia. The focus of the analysis is on the relative impact of BBOA CCN on CDNC, supersaturation and the contributions of aerosol number and hygroscopicity on the resulting CDNC.*

See Section 3.8, pages 35-37 of the current file

General / major comments:

1. The authors present the plume from the Balkans as a representative case of more aged biomass burning aerosol. This is certainly true, but it is also possible that the type of biomass burned at the Balkans can be different from the Greek plumes. It is well known that the properties of biomass burning aerosol from different types of fuels can differ significantly, so I would expect it to be difficult to separate the effect of ageing vs. the type of fuel being burned. The authors should comment on this. In general, the generalizability of the reported results to areas outside the eastern Mediterranean should be discussed in the manuscript.

Response*: We never said that the type of biomass burning at different locations is the same; indeed, a detailed analysis of the different kind of each fire event spectra can be found in the study of Bougiatioti et al. (2014) and the respective supplementary material. Nevertheless, in that study the organic aerosol derived mainly from the aging of the biomass burning aerosol (OOA-BB) had a similar profile, regardless of the BBOA it was derived from. What we wanted to point out was the effect that aging and atmospheric processing may have on the hygroscopicity. Nevertheless, as pointed out by the other anonymous referees as well, more details and information concerning the fire events will be given in the revised version of the manuscript.*

See page 24, lines 1075-1081 of the current file

2. I am not convinced, at least based on the presented discussion, that the differences in condensation and coagulation are the primary factors explaining the different mixing states of the smaller and larger particles. Wouldn't it be a more plausible explanation that the smaller particles that make their way to Finokalia have originated primarily from secondary sources while the larger particles have a more important primary particle component? This smaller variability in the sources of the smaller as compared with larger particles could also potentially explain the observed smaller variability in the hygroscopicity distribution as well. In general, the discussion of the coagulation and the condensation is unquantitative and thus sloppy, for instance I suspect the authors in refer only to self-coagulation when they talk about "coagulation" in general in the text. It is well known that coagulation is more efficient for particles with different sizes, acting therefore primarily as a loss mechanism for the smaller particles, while being similar to condensation from the perspective of the large particles. This

section of the discussion of the results on p. 21555-21556 needs to be revised, along with the corresponding discussion in the conclusions section.

***Response**: The issue about the differences in condensation/coagulation explaining the differences in the mixing state of the different particle sizes is raised by all referees. We completely agree that the path of secondary formation of the smaller particles during the transport of the air masses is the most plausible explanation of the different mixing state. This will be included in the discussion, along with the estimate of the composition of the different particle sizes.*

See pages 29-30, lines 1286-1303 of the current file

Minor / technical comments:

3. When giving the kappa values throughout the manuscript (particularly in Tables 1- 3), please pay attention to the number of significant digits given in light of experimental variability and error. Is it really possible to constrain kappa within 0.001-0.01? If yes, please provide justification why you think so.

***Response**: Good point. The significant digits were derived from the statistical analysis of the data. All kappa values are now provided with 2 significant digits.*

See page 48 of the current file

4. The quality of the figures is in many cases insufficient and the fonts and linewidths chosen are too small. Please revise all figures keeping in mind the readability of the figures in typical ACP print versions.

***Response**: We would link to thank the reviewer for pointing out this issue. Depending on the amount of information on each figure, fonts and linewidths will be the largest possible to ensure good readability of the figures.*

5. P. 21541, line 12: Please quantify what you mean by “smaller” particles.

***Response**: Good point. Done. The text now reads “particle sizes smaller than 80 nm”.*

6. P. 21541, line 23: “BBOA” not defined before used. Please revise.

***Response**: Done.*

7. P. 21541, line 23: “enhancements” compared to what? Please clarify.

***Response**: Done. The text now reads “..with enhanced CCN concentrations than the ones before the arrival of the smoke plume, ranging between…”*

See page 26, lines 1140-1142 of the current file

8. P. 21542, line 20: “impact” -> impacting

***Response**: Done.*

9. P. 21542, line 25: What do you mean by bb aerosol being “half of ammonium sulphate”? I presume you mean the hygroscopicity parameter, but please clarify.

***Response**: Done.*

See page 18, lines 806-807 of the current file

10. P. 21550, line 1: “CALPSO” -> CALIPSO

***Response**: Done.*

~~Influence of biomass burning on CCN number and hygroscopicity~~Biomass burning impact on CCN number, hygroscopicity and cloud formation during summertime in the ~~eastern~~ Eastern Mediterranean

A. Bougiatioti[1,2,3], S. Bezantakos[4,5], I. Stavroulas[3], N. Kalivitis[3], P. Kokkalis[2,11], G. Biskos[6,7], N. Mihalopoulos[3,7,10], A. Papayannis[2], A. Nenes[1,8,9,10]

[1]School of Earth and Atmospheric Sciences, Georgia Institute of Technology, Atlanta, GA, USA
[2]Laser Remote Sensing Unit, National Technical University of Athens, Zografou, Athens, Greece
[3]ECPL, Department of Chemistry, University of Crete, Voutes, 71003 Heraklion, Greece
[4]Department of Environment, University of the Aegean, Mytilene, 81100, Greece
[5]Institute of Nuclear Technology and Radiation Protection, NCSR "Demokritos", 15310 Ag. Paraskevi, Athens, Greece
[6]Faculty of Civil Engineering and Geosciences, Delft University of Technology, Delft 2728 CN, The Netherlands
[7]Energy Environment and Water Research Center, The Cyprus Institute, Nicosia 2121, Cyprus
[8]School of Chemical & Biomolecular Engineering, Georgia Institute of Technology, Atlanta, GA, USA
[9]Institute of Chemical Engineering Sciences (ICE-HT), FORTH, Patras, Greece
[10]IERSD, National Observatory of Athens, P. Penteli 15236, Athens, Greece
[11]IAASARS, National Observatory of Athens, P. Penteli 15236, Athens, Greece

Abstract

This study investigates the concentration, cloud condensation nuclei (CCN) activity and hygroscopic properties of particles influenced by biomass burning in the eastern Mediterranean and their impacts on cloud droplet formation. Air masses sampled were subject to a range of atmospheric processing (several hours up to 3 days). Values of the hygroscopicity parameter, κ, were derived from ~~cloud condensation nuclei (~~CCN~~)~~ measurements and a Hygroscopic Tandem Differential Mobility Analyzer (HTDMA). An Aerosol Chemical Speciation Monitor (ACSM) was also used to determine the chemical composition and mass concentration of non-refractory components of the submicron aerosol fraction. During fire events, the increased organic content (and lower inorganic fraction) of the aerosol decreases the ~~hygroscopicity parameter,~~values of κ, for all particle sizes. ~~The reason, however, for this decrease was not the same for all size modes; smaller particle sizes appeared to be richer in less hygroscopic, less CCN-active components due to coagulation processes while larger particles become less hygroscopic during the biomass burning events due to condensation of less hygroscopic gaseous compounds. In addition, smaller particles~~ Particle sizes smaller than 80 nm exhibited considerable chemical dispersion (where hygroscopicity varied up to 100% for particles of same size); larger particles, however, exhibited considerably less dispersion owing to the effects of condensational growth and cloud processing. ~~aging and retained high levels of CCN activity. These conclusions are further supported by the observed mixing state determined by the HTDMA measurements.~~ ACSM measurements indicate that the bulk composition reflects the hygroscopicity and chemical nature of the largest particles (having a diameter of ~100 nm at dry conditions) ~~and a large fraction of the CCN concentrations~~ sampled. Based on Positive Matrix Factorization (PMF) analysis of the organic ACSM spectra, CCN concentrations follow a similar trend with the ~~BBOA~~ biomass burning organic aerosol

(BBOA) component, with ~~enhancements of CCN~~ the former being enhanced between 65 and 150% (for supersaturations ranging between 0.2 and 0.7%) with the arrival of the smoke plumes~~ in biomass burning plumes ranging between 65 and 150%, for supersaturations ranging between 0.2 and 0.7%~~. Using multilinear regression of the PMF factors (BBOA, OOA-BB and OOA) and the observed hygroscopicity parameter, the inferred hygroscopicity of the oxygenated organic aerosol components is determined. ~~we determine the hygroscopicity of the prime organic aerosol components (BBOA, OOA-BB and OOA); it is found that the total organic hygroscopicity is very close to the inferred hygroscopicity of the oxygenated organic aerosol components. Finally,~~ We find that the transformation of freshly-emitted biomass burning (BBOA) to more oxidized organic aerosol (OOA-BB) can result in a ~~two-fold~~twofold increase of the inferred organic hygroscopicity~~.~~; ~~Almost~~ about 10% of the total aerosol hygroscopicity is related to the two biomass burning components (BBOA and OOA-BB), which in turn contribute almost 35% to the fine-particle organic water of the aerosol. ~~This is important as organic water can contribute to the atmospheric chemistry and the direct radiative forcing.~~ Observation-derived calculations of the cloud droplet concentrations that develop for typical boundary layer clouds conditions suggest that biomass burning increases droplet number, on average by 8.5%. The strongly sublinear response of clouds to biomass burning (BB) influences is a result of strong competition of CCN for water vapor, which results in very low maximum supersaturation (0.08% on average). Attributing droplet number variations to the total aerosol number and the chemical composition variations shows that the importance of chemical composition increases with distance, contributing up to 25% of the total droplet variability. Therefore, although BB burning may strongly elevate CCN numbers, the impact on droplet number is limited by water vapor availability and depends on the aerosol particle concentration levels associated with the background.

1. Introduction

Globally, biomass burning (BB) is a major source of atmospheric aerosols (Andreae et al., 2004). In the eastern Mediterranean, up to one third of the dry submicron aerosol mass during the summer period consists of highly oxidized organic compounds (Hildebrandt et al., 2010). During July-September, biomass-burning aerosol originates from long-range transport from Southern Europe and countries surrounding the Black Sea (Sciare et al., 2008). Bougiatioti et al. (2014) showed that of the total organic aerosol (OA), about 20% is freshly-emitted biomass burning organic aerosol (BBOA), 30% is oxidized, processed OA originating from BBOA (BB-OOA), and the remaining 50% is highly oxidized aerosol that results from extensive atmospheric aging. Hence, in term of organic mass, during time periods of high biomass burning activity, ~~up to~~at least 50% of the aerosol can be ~~influenced by these~~ attributed to BB emissions.
Aerosol liquid water content (LWC) is a key medium for atmospheric chemistry that also drives the partitioning of soluble organic vapors to the particle phase (Carlton and Turpin, 2013). LWC is a prime modulator of aerosol direct radiative forcing (e.g., Pilinis et al., 1995), and by promoting secondary aerosol formation it can influence aerosol

mass and number, that impacts both on the aerosol direct and indirect effect (Kanakidou et al., 2005).

Biomass burning aerosol particles have the potential to act as cloud condensation nuclei (CCN), thereby impacting on cloud properties and climate. Modeling studies suggest that BB is a significant global source of CCN number (Spracklen et al., 2011). ~~It is therefore important to understand how biomass burning contributes to CCN and aerosol hygroscopicity and how it evolves in the atmosphere.~~ Laboratory and field studies ~~suggest~~ have shown that ~~the water-soluble component of~~ biomass burning aerosol is highly hygroscopic and water-soluble, exhibiting up to about half the water uptake capacity of ~~about half of~~ ammonium sulfate (Asa-Awuku et al., ~~2010~~2008; Cerully et al., 2014). Engelhart et al. (2012) found that freshly emitted BBOA displays a broad range of hygroscopicity (κ parameter from 0.06 to 0.6) that considerably reduces after just a few hours of photochemical ~~processing~~aging, to a κ value of 0.2±0.1 (Petters and Kreidenweis, 2007). Few studies, however, focus on the hygroscopicity of ambient BB aerosol ~~for a range~~as a function of atmospheric ~~aging~~age extending out to a few days. Relatively few studies also go beyond CCN to calculations of droplet number (e.g., Roberts et al., 2003), and even fewer studies characterize the relative role of aerosol number and chemical composition (hygroscopicity) variability to the predicted droplet number variability in clouds formed from BB-influenced masses. These issues are important, because the supersaturation that develops in clouds is not known beforehand, nor constant, but rather a strong function of the CCN levels and cloud dynamical forcing (updraft velocity).

In the current study we focus on the hygroscopicity, CCN ~~activity and hygroscopicity~~ concentrations and resulting droplet formation characteristics (droplet number and cloud supersaturation) ~~of ambient aerosol~~ associated with air masses influenced by summertime biomass burning events in the eastern Mediterranean ~~during summertime~~. The ~~events were not local and~~ smoke-laden air masses sampled were subject to a range of atmospheric processing (several hours up to 3 days), identified using remote sensing techniques (Moderate Resolution Imaging Spectroradiometer, Kaufman and Remer, 1994; Cloud-Aerosol Lidar with Orthogonal Polarization, Winker et al., 2009, Mamouri et al., 2012), backtrajectory analysis and other in-situ chemical metrics. ~~. Smoke plumes sampled are identified by the Moderate Resolution Imaging Spectroradiometer (MODIS) (Remy and Kaiser, 2014) onboard the Terra and Aqua satellites and the laser remote sensing (lidar) system on board the space-borne Cloud-Aerosol Lidar with Orthogonal Polarization (CALIOP) platform (Winker et al., 2009; Mamouri et al., 2012).~~ Values of the hygroscopicity parameter, κ, were derived from CCN and HTDMA measurements and linked to distinct chemical constituents identified with Positive Matrix Factorization of the chemical constituents measured with ~~while the chemical composition and mass concentration of non-refractory components of the submicron aerosol fraction was studied using~~ an Aerosol Chemical Speciation Monitor (ACSM). Finally, the observations are used to predict the cloud droplet number and supersaturation formed in clouds that develop in each air mass, focusing on the contribution of aerosol number and hygroscopicity to the predicted droplet number variability. ~~The originality of our study relies on the fact that, to our knowledge,~~ This is one of the very few field studies ~~were able to focus on the hygroscopicity of ambient~~

~~biomass burning aerosol for a range of atmospheric aging, which is addressed here.~~that use in-situ observations to i) unravel the contributions of composition and aerosol size to BB CCN distributions and their impacts on cloud droplet number, ii) quantify the ~~The study also examines the~~ contributions of biomass burning constituents to aerosol ~~different organic aerosol components to the overall~~ hygroscopicity and liquid water in the region. ~~which in turn may contribute to the aerosol liquid water content (LWC), as the potential of organic gases to partition to LWC is sometimes greater than the potential to partition to particle-phase organic matter (Carlton and Turpin, 2013). LWC is important as it has a direct effect on aerosol particles by enhancing scattering but also can contribute to the indirect effect by promoting secondary aerosol formation (Nguyen et al., 2013; Guo et al., 2015).~~

2. Experimental Methods

2.1 Sampling site and period

The measurements were performed at the Finokalia station (35º32'N, 25º67'E; http://finokalia.chemistry.uoc.gr) of the University of Crete, which is part of the Aerosols, Clouds, and Trace gases Research Infrastructure Network (ACTRIS; http://www.actris.net/). More details about the sampling site ~~have been~~are provided by Mihalopoulos et al. (1997) and Sciare et al. (2003). ~~Measurements~~ Although measurements took place from mid-August to mid-November 2012, the focus of our analysis ~~however~~ involves the periods of intense biomass burning influence, August to September 2012. BB plumes sampled were fresh, originating from the Greek islands and mainland (transport time 6-7 h) but also from long-range transport from the Balkans (transport time > 1 day) as determined by using HYSPLIT backtrajectory analysis as shown in detail in Bougiatioti et al. 2014 combined with the hot spots/fire data from MODIS/Fire Information for Resource Management System (FIRMS; Remy and Kaiser, 2014).

2.2 Instrumentation and methodology

Chemical composition and mass concentration of non-refractory components (ammonium, sulfate, nitrate, chloride and organics) of the submicron aerosol fraction was provided by an Aerodyne Research Aerosol Chemical Speciation Monitor (ACSM; Ng et al., 2011) with a temporal resolution of 30 minutes. More details of the ACSM measurements and subsequent analysis can be found in Bougiatioti et al. (2014). Total absorption measurements provided the black carbon (BC) concentrations by a seven-wavelength aethalometer (Magee Scientific, AE31). From the BC measurements and using the approach of Sandradewi et al. (2008) the wood-burning and fossil fuel contribution to the total BC concentrations were calculated, using an absorption exponent of 1.1 for fossil fuel burning and 1.86 for pure wood burning. The aerosol particle size distributions from 9 to 850 nm were ~~monitored~~measured with a 5-min resolution by a custom-built scanning mobility particle sizer (SMPS; TROPOS-type, Wiedensohler et al., 2012) equipped with a condensation particle counter (CPC; TSI model 3772; ; Stolzenburg and McMurry, 1991)~~ that provides measurements of the aerosol size distribution every 5 min~~. Sample humidity was regulated below the relative

humidity of 40% with the use of Nafion® dryers in both aerosol and sheath flow and the measured umber size distributions were corrected for diffusional particle losses (Kalivitis at al. 2015).

A Continuous Flow Stream-wise Thermal Gradient CCN Chamber (CFSTGC; Roberts and Nenes, 2005) was used in parallel with a Hygroscopic Tandem Differential Mobility Analyzer (HTDMA; Rader and McMurry, 1986) to measure the CCN number, activity and hygroscopicity of ambient aerosol for supersaturated (0.1-0.7%) and subsaturated conditions (relative humidity, RH=86%), respectively. The whole system, which is illustrated in Figure 1, sampled air with a total flow-rate of 1.8 L min^{-1}. After passing through a ~~nafion~~ Nafion dryer (MD-110-12S-2, Perma Pure LLC, RH<30%) the dried particles were selected based on their electrical mobility by a Differential Mobility Analyzer (DMA-1;TSI Model 3080; Knutson and Whitby, 1975). The sheath flow and classified aerosol outlet flow of DMA-1 were 10.8 and 1.8 L min^{-1}, respectively, while the mobility diameter was changed every 6 minutes between 60, 80, 100 and 120 nm. The classified aerosol from DMA-1 was then split into two streams. The first stream was passed through a ~~nafion~~Nafion-tube humidity exchanger where its RH was increased to 86%. The size distribution of the RH-conditioned particles was determined by a second DMA (DMA-2; custom-made DMA using a closed-loop sheath flow with RH control; Biskos et al., 2006; Bezantakos et al., 2013) coupled with a Condensation Particle Counter (CPC, TSI Model 3772~~; Stolzenburg and McMurry, 1991) to measure the total number concentration of each classified particle size~~. The RH in both the aerosol and the sheath flow in DMA-2 was controlled by PID controllers to within ~~a~~ ±2% accuracy. Both DMAs in the HTDMA system were calibrated with Polystyrene Latex (PSL) spheres. The other classified stream was introduced into the CFSTGC to measure the CCN activity of particles. The CFSTGC was operated in Scanning Flow CCN Analysis (SFCA) mode (Moore and Nenes, 2009), in which the flow rate in the growth chamber changes over time, while a constant streamwise temperature difference is applied. This causes supersaturation to change continuously, allowing the rapid and continuous measurement of CCN spectra with high temporal resolution. The SFCA cycle used involved first increasing the flow rate linearly between a minimum flow rate (Q_{min} ~ 300 cm^3 min^{-1}) and a maximum flow rate (Q_{max} ~ 1000 cm^3 min^{-1}) over a ramp time of 60 seconds. The flow was maintained at Q_{max} for 10 seconds and then linearly decreased to Q_{min} over 60 s. Finally, the flow rate was held constant at Q_{min} for 10 s and the scan cycle was repeated. The activated droplets in the CFSTGC were counted and sized at the exit of its growth chamber with an Optical Particle Counter (OPC) that detects droplets and classifies them into 20 size bins with diameter ranging from 0.7 to 10 μm every 1 s.

The water vapor supersaturations developed in the CFSTGC during an SFCA cycle were characterized ~~overall performance of the system was investigated~~ with ammonium sulfate calibration aerosol following the procedure of Moore and Nenes (2009). In brief, an ammonium sulfate solution was atomized, dried, charge-neutralized and classified by DMA-1. The resulting monodisperse aerosol flow was split between DMA-2 and the CFSTGC, operating in SFCA mode and with a CFSTGC streamwise temperature difference of ΔT=5 K. From this setup, we obtain the instantaneous concentrations of the classified aerosol and the resulting CCN during the SFCA flow cycles. ~~resulting in~~

~~total number at each size as well as the corresponding CCN~~. ~~This~~ The ratio of CCN to total aerosol number gives ~~provided~~ the activation ratio, R_a, which varies with the instantaneous volumetric flow rate, Q, in the CFSTGC. Using data from multiple SFCA flow cycles, R_a is then ~~which was plotted against the instantaneous flow rate and~~ fit to a sigmoid function that depends on Q:

$$R_a \equiv \frac{CCN}{CN} = a_o + \frac{a_1 - a_0}{1 + (Q/Q_{50})^{-a_2}} \qquad (1)$$

where a_0, a_1, a_2 and Q_{50}, are constants which describe the minimum, maximum, slope and inflection point of the sigmoidal, respectively. The "critical flow rate", Q_{50}, corresponds to the instantaneous flow rate that produces a level of supersaturation, s, required to activate the measured monodisperse aerosol. s is determined from the size of the classified aerosol using Köhler theory (Moore et al., 2012a).

~~. The point at which half of the particles of the selected size act as CCN corresponds to a "critical flow" and the instantaneous supersaturation inside the chamber (critical supersaturation) of the classified ammonium sulfate. Repeating the procedure for several sizes of classified ammonium sulfate results in the calibration curve.~~

~~Supersaturation in the CFSTGC were calibrated in terms of the CCNC streamwise temperature difference (ΔT=5 K), the instantaneous flow rate and the overall flow rate range. Sigmoidal activation curves of CCN versus flow rate are obtained, and the inflection point of the sigmoid is used as the critical activation flow, Q_{50}, rate which corresponds to the critical supersaturation S_c (hence instrument supersaturation) above which particles act as CCN. The humidification in the DMA-2 was also evaluated by the growth factor measured for the calibration $(NH_4)_2SO_4$. CCN activation is characterized by the CCN to CN ratio (activation ratio), R_a, which is a function of instantaneous flow rate during a flow cycle. R_a data were fit to the sigmoidal equation: The implementation of Köhler theory presented by Moore et al. (2012a) is used to convert the critical activation flow in terms of critical supersaturation~~.

Repeating the procedure for many sizes of classified ammonium sulfate results in the SFCA calibration curve, which gives the supersaturation in the CFSTGC as a function of flow rate (i.e Q_{50} vs. s) throughout an SFCA flow cycle. Absolute uncertainty of the calibrated CCNC supersaturation is estimated to be ±0.04% (Moore et al., 2012a; 2012b). ~~This process is repeated for many calibration aerosol sizes to obtain a comprehensive calibration.~~

In our instrument setup, R_a can change either from variations in the size of the monodisperse aerosol, d_p, or the instrument supersaturation, s (or flow rate, Q). The independently varied parameter is indicated hereon in parentheses in front of the activation ratio, e.g., $R_a(Q)$, $R_a(s)$, $R_a(d_p)$ for R_a as a function of Q, s and d_p, respectively.

Analysis of R_a obtained for our experimental setup for ambient particles samples provide very important information on the activity and chemical mixing state of the CCN. This is carried out as follows. For every particle size d_p set by the DMA-1, $R_a(Q)$, is measured at every instant in the CFSTGC according to Eq.1. Typically $a_0 << a_1$; given that Q and s are related through the calibration, $R_a(Q)$ data can be transformed to $R_a(s)$ as:

$$R_a(s) = \frac{E}{1+\left(\frac{s}{s^*}\right)^C} \quad (2)$$

where s, s^* correspond to Q, Q_{50} of the monodisperse aerosol. E, C are parameters determined from fitting. According to Cerully et al., (2011), $R_a(s)$ represents a cumulative distribution of critical supersaturation for particles with dry diameter d_p; Köhler theory can then be applied to express $R_a(s)$ in terms of the hygroscopicity parameter $R_a(\kappa)$:

$$R_a(\kappa) = \frac{E}{1+\left(\frac{\kappa}{\kappa^*}\right)^{C/2}} \quad (3)$$

where $\kappa = \frac{4A^3}{27 d_p^{\,3} s^2}$ is the dependence of κ on d_p and s, $A = \frac{4M_w\sigma_w}{RT\rho_w}$ is the Kelvin parameter, whereas M_w, σ_w and ρ_w are respectively the molar mass, the surface tension and the density of water, R is the universal gas constant, and T is temperature. In equations 2, 3, s^* and κ^* correspond to the characteristic critical supersaturation and hygroscopicity parameter of the monodisperse aerosol, respectively and correspond to the most probably values of the parameters (Cerully et al., 2011). From Equation 3, the probability distribution function for κ, $p^s(\kappa)$, can be derived for the ambient monodisperse aerosol (Cerully et al., 2011):

$$p^s(\kappa) = \frac{1}{E}\frac{dR_a(\kappa)}{d\kappa} = -\frac{\frac{C}{\kappa^* 2}\left(\frac{\kappa}{\kappa^*}\right)^{\frac{C}{2}-1}}{\left(1+\left(\frac{\kappa}{\kappa^*}\right)^{\frac{C}{2}}\right)^2} \quad (4)$$

Analysis of $p^s(\kappa)$ can provide a direct measure of the chemical heterogeneity of the CCN population. For this, we adopt the metric of chemical dispersion, $\sigma(\kappa)$, introduced by Lance (2007) and further developed in Cerully et al. (2011) and Lance et al. (2013):

$$\sigma^2(\kappa) = \frac{\int_0^1 (\kappa-\kappa^*)^2 p^s(\kappa)d\kappa}{\int_0^1 p^s(\kappa)d\kappa} \quad (5)$$

$\sigma(\kappa)$ is the square root of variance about κ^*; as the chemical heterogeneity of the CCN increases, the distribution of κ broadens, and $\sigma(\kappa)$ becomes larger so that the range in CCN hygroscopicity is given by $\kappa^* \pm \sigma(\kappa)$.

~~R_a can also be expressed as a function of supersaturation using the calibration of Q vs S as follows:~~

~~where E is the maximum fraction of particles that activate at a given supersaturation, S is the instrument supersaturation and S^* is the characteristic critical supersaturation at which half of the classified CCN activate. In the term of equation 2, R_a represents a~~

~~cumulative distribution of critical supersaturation for particles with dry diameter d_p (Cerully et al., 2011). Köhler theory can then be applied to transform $R_a(s)$ into accumulative distribution of hygroscopicity parameter $R_a(\kappa)$:~~

~~where M_w, σ_w and ρ_w are respectively the molar mass, the surface tension and the density of water, R is the universal gas constant, and T is temperature. For every critical supersaturation there is a corresponding characteristic hygroscopicity parameter, κ^*, and the probability distribution function for κ, $p^s(\kappa)$ can provide the chemical dispersion, which describes the degree of chemical heterogeneity of the CCN population (Cerully et al., 2011).~~

Particle water uptake at sub-saturated conditions in the Nafion-tube humidity exchanger and DMA-2 was also evaluated by the growth factor measured for the calibration $(NH_4)_2SO_4$. Particle hygroscopic growth at sub-saturated conditions (g_i) is obtained by:

$$g(RH) = \frac{d_m(RH)}{d_p} \tag{6}$$

where $d_m(RH)$ and d_p are the geometric mean mobility diameters of the sampled particles at the hydrated state (i.e. at RH=86%) as measured by DMA-2 and the CPC, and at the dry state selected by DMA-1 (RH< 30%), respectively. Particle size distributions at 86% RH were inverted using the TDMAfit algorithm (Stolzenburg and McMurry, 1988) which is also capable of distinguishing between internally and externally mixed aerosols (e.g. Bezantakos et al., 2013).

Hygroscopicities determined from the CCN measurements are differentiated by corresponding values from the HTDMA measurements by including and index CCN, HTDMA, respectively (e.g. κ_{HTDMA}, κ_{CCN}). ~~The corresponding~~ κ_{HTDMA} ~~values~~ is calculated from the HTDMA-measured ~~at~~ sub-saturated ~~conditions are calculated~~hygroscopic growth factors using:

$$\kappa_{HTDMA} = (g(RH)^3 - 1)\left(\frac{\exp\left(\frac{A}{g(RH) * d_p}\right)}{\frac{RH}{100\%}} - 1\right) \tag{7}$$

with A being ~~already~~ the Kelvin paraeter defined in Equation 3. The exponential term of this equation (i.e. the Kelvin term) is used to account for curvature effects on vapor pressure.

An average value of the hygroscopic parameter at each dry particle size, d_p , which is representative of the hygroscopic properties of the entire particle population is obtained as follows:

$$\overline{\kappa_{HTDMA}} = \int_{g_{\min}}^{g_{\max}} \kappa(g_{(RH)})\, p(g_{(RH)})\, dg_{(RH)} \tag{6}$$

where $\kappa(g_{(RH)})$ is obtained from the growth factor probability distribution using equation 5 and $p(g_{(RH)})$ is the probability of each growth factor. g_{min}, g_{max} are the minimum and maximum growth factors, respectively, obtained from the growth factor probability distribution and represent the minimum and maximum g with non-zero probability value.

~~Chemical composition and mass concentration of non-refractory components (ammonium, sulfate, nitrate, chloride and organics) of the submicron aerosol fraction was provided by an Aerodyne Research Aerosol Chemical Speciation Monitor (ACSM; Ng et al., 2011) with a temporal resolution of 30 minutes. More details of the ACSM measurements can be found in Bougiatioti et al. (2014). Total absorption measurements provided the black carbon (BC) concentrations by a seven-wavelength aethalometer (Magee Scientific, AE31). From the BC measurements and using the approach of Sandradewi et al. (2008) the wood-burning and fossil fuel contribution to the total BC concentrations were calculated, using an absorption exponent of 1.1 for fossil fuel burning and 1.86 for pure wood burning. The aerosol particle size distributions from 9 to 850 nm were monitored by a custom-built scanning mobility particle sizer (SMPS; TROPOS-type, Wiedensohler et al., 2012) equipped with a condensation particle counter (CPC; TSI model 3772) that provides measurements of the aerosol size distribution every 5 min.~~

To support the *in situ* instruments, we used space-borne laser remote sensing (lidar) data from CALIOP (Mamouri et al., 2009; Winker et al., 2009) to characterize the plumes emerging from the fire hot spots. The fire plume originating from ~~the~~ any location can be tracked by HYSPLIT back-trajectory analysis (Bougiatioti et al., 2014) and lidar observations can be used to check the presence of aerosol layers and aerosol types. Optical confirmation of the smoke plumes is provided by MODIS and FIRMS as shown in the supplementary material of Bougiatioti et al. 2014. ~~CALIOP is also able to provide the vertical profiles of different types of aerosols, as well as the optical properties of clouds over the globe with unprecedented spatial resolution since June 2006 (Winker et al., 2009).~~

3. Results and Discussion

3.1 Identifying periods of biomass burning influence

Bougiatioti et al. (2014) identified the BB events analyzed here by the time evolution of absorption enhancements (BC) in the aerosol, which was further verified by FIRMS and back-trajectory analysis. During these events mass spectrometric biomass burning tracers (i.e. fragments m/z=60 and 73) also exhibited elevated levels. Clear biomass burning contribution was identified by source apportionment using Positive Matrix Factorization (PMF) analysis for four distinct events. The BB events considered include a severe fire event that burned most of the island of Chios (19–21 August), an extensive wildfire at the Dalmatian Coast in Croatia resulting in smoke plumes that spread across the Balkans during the period 28–30 August, and, less extensive fires on the Greek islands of Euboea (3-5 September) and Andros (12-13 September). All fire events exhibited discrete BBOA profiles depending on the biomass burning fuel, as presented in detail by Bougiatioti et al. (2014). Nevertheless, the organic aerosol derived from the aging of the biomass burning aerosol (OOA-BB) identified for all events had a similar profile, regardless of the BBOA it was derived from (Bougiatioti et al. 2014). Transport time estimate and backtrajectory analysis were conducted with the Plume Arrival (h) from Base Time graphics with the help of the HYSPLIT model (www.arl.noaa.gov/hysplit.php).

MODIS and CALIOP measurements confirm the validity of the Bougiatioti et al. (2014) analysis, by clearly showing the origin, transport path and characteristics of the biomass burning plume from the Chios fire on 18 and 19 August 2012, respectively. Indeed, in Figure 2a we show the MODIS true color image showing the plume emerging from the Chios fires on 18 August ~~1992~~ 2012 as obtained during its 9.39 UTC overpass over Greece (Kyzirakos et al., 2014). The blue and red lines delineate the ground track of the CALIPSO satellite during its overpass over Crete several hours later on 19 August 2012 (the first between~~on~~ 00:27-00:40 and the second between11:34-11:47 UTC~~, respectively)~~; the red star shows the sampling site at Finokalia station. The CALIPSO vertical profiles of the aerosol backscatter coefficient (in $km^{-1}sr^{-1}$) at 532 and 1064 nm for the two overpasses ~~(at 00:27-00:40 and 11:34-11:47 UTC)~~ are shown in Figure 2b (left-hand side) together with the corresponding linear particle depolarization ratio at 532 nm obtained between 00:27:30-00:40 UTC (right-hand side). Comparing the midnight and the daytime aerosol backscatter profiles in Figure 2b, we observe that the midnight values are 3-4 times lower than the daytime ones for altitudes up to 3 km height. In addition, the daytime observations show a discrete aerosol layer bel~~l~~ow 1.5 km. As for the linear particle depolarization ratio it shows a mean value of 19% (up to 1.25 km height) and less than 6-10% (1.25-2 km). Finally, we made use of the classification scheme of the CALIPSO data (Omar et al., 2009) to classify the different subtypes of aerosols in the plume captured during its first overpass over Crete on 19 August 2012 (00:27-00:40 UTC). This classification scheme, based on the optical and microphysical properties of the sampled aerosols indeed reveals the presence of a mixture of smoke, polluted dust and marine particles observed below a 3 km altitude (black color for smoke, brown for polluted dust and blue for marine) as shown in Figure 2c, within the depicted area between 39ºN, 24.1ºE-37ºN, 23.4ºE, just NW of the Finokalia station and along the CALIPSO ground track. According to this classification, over Crete the presence of polluted dust (mixed with smoke and marine aerosols) prevails within the marine boundary layer, which for Finokalia is approximately 1 km (Kalivitis et al., 2007), extending up to 0.8-1.2km height. This implies that for the 00:27–00:40 UTC time slot, the BB aerosols sampled by the ground-based in situ measurements at Finokalia would contribute less (due to dilution) to the global aerosol mass loading than, if measured, over the Western Crete.

3.2 PM_1 composition

The average mass concentration for the whole measurement period (mid-August to mid-November 2012), based on the ACSM measurements combined with BC from the aethalometer was 9.2±4.8 μg m^{-3}. The corresponding ~~average~~ median concentrations for the main aerosol constituents were ~~2.87±1.85~~3.56, ~~0.91±0.71~~1.31, ~~2.33±1.05~~ 3.03 and ~~0.41±0.18~~0.47 μg m^{-3} for sulfate, ammonium, organics and BC respectively. Figure 3 represents the time series of the major submicron species where it can be seen that during the fire events the contribution of organics and BC increased substantially (from 34.9 to 46.5% for organics and from 6.1 to 9.5% for BC) with a simultaneous reduction of that of sulfate. Source apportionment clearly shows that these increases are related to BB influences (Bougiatioti et al. 2014). During all BB events there is a clear dominance of wood burning over fossil fuel contributions to BC.

The wood burning component of BC is also provided as a reference, depicting the enhanced contribution of biomass burning during the highlighted events.

Based ~~on Köhler theory and the calculation of the critical supersaturation,~~ the size-resolved CCN activity measurements and the inferred hygroscopicity parameter κ of the aerosol (Equation 3), it is evident that the changes in the organics and sulfate mass fractions will also influence the CCN concentrations, activation fractions and hygroscopicity. As the ACSM provides bulk submicron chemical composition and thus, is not able to capture any sized-dependent chemical composition, the size-resolved CCN activity measurements are able to resolve distinct CCN activity and mixing state of the different particle sizes. These aspects are thoroughly investigated in the following sections.

3.3 CN and CCN number concentrations and biomass burning events

~~During~~ For all four events of biomass burning-influenced air masses arriving at Finokalia, the observed aerosol number concentration ~~for all particle sizes that were measured~~ increased considerably, regardless of size. The increases are quantitatively expressed using averaged data from at least 6 hours prior to the arrival time of the BB smoke. For ~~most of the events and especially for the larger~~ particle sizes above 100 nm, BB increased concentrations ~~exhibited an increase that for~~ by 65% for ~~the case of~~ the Chios fire ~~was around 65%~~, around 50% for the Croatia fire ~~around 50%~~, 88% for the Euboea fire ~~88%~~ and about 150% for the Andros fire ~~around 150%~~. ~~This~~ Less pronounced increases was ~~also observed~~seen for the smaller particle sizes ~~but was less pronounced~~. The corresponding impacts on CCN concentrations for the classified aerosol are shown in Figure 4 for all fire events. ~~represents the CCN concentrations of the classified aerosol at the centroid mobility diameter measured, for the four identified fire events; (a) Chios, (b) Croatia, (c) Euboea and (d) Andros.~~ Concentrations are given at the ~~point of critical activation flow Q_{50} of the SFCA, corresponding to the instantaneous~~characteristic supersaturation, s^*, ~~for each particle size, as described in detail in section 2.2~~of the monodisperse CCN as classified by DMA-1 (Section 2.2). Within each event, s^* did not vary by more than 13.6%; therefore most of the variability in CCN number can be attributed to variations in the size distribution, rather than shifts in the chemical composition (i.e., s^*).

As expected, smaller particles exhibit ~~the~~ a higher critical supersaturation (Bougiatioti et al., 2011). ~~It can also be seen that d~~During ~~the~~ periods with smoke influence, critical supersaturations ~~are higher~~tend to increase, indicating that particles ~~-~~associated with BB are less effective CCN compared to those of the background aerosol. ~~do not activate so readily~~. ~~In order to see~~To quantify the direct influence of biomass burning to particle and CCN number concentrations~~, along with the CCN concentrations~~ we studied the concentration of the BBOA component, identified by PMF analysis of the ACSM mass spectra (Bougiatioti et al., 2014). The BBOA concentration time series depicts the arrival time of the smoke ~~plume~~ and the ~~magnitude of the event~~intensity of the BB influence~~, based on the measured concentration. More details about the PMF analysis can be found in Bougiatioti et al. (2014)~~.

The data shown in Figure 4 indicates that during the majority of the identified biomass burning events, CCN concentrations for the larger particles sizes increase, ~~tracking~~ and

follow the BBOA trend. This increase was more pronounced, depending on the proximity of the fire and therefore, the travel time of the air masses. ~~Similar observations have been reported by~~ Rose et al. (2010) also observed increases in CCN during a biomass burning event near the mega-city Guangzhou, China~~ during the PRIDE-PRD2006 campaign~~, where CCN number concentrations at ~~lower supersaturations of~~ s=0.068 and 0.27%, ~~CCN number concentrations were higher than the study average~~increased by 90 and 8%, respectively~~, which was attributed to the larger average particle sizes~~. The same study attributed these changes to increases in the particle size when BB influence was present.

Of all particle sizes examined, it appears that those having mobility diameter of 60 nm exhibit the least variability in terms of CCN number concentration before and during the BB influence (Figure 4, open circles). The concentrations however of the classified aerosol significantly increase during the BB event from Croatia (Figure 4b).~~It can also be seen that that the particles that appear to be less influenced for all of the events, are those having a diameter of 60 nm. Nevertheless, for these particles it can be seen that following the influence of the Croatia fire (Figure 4b), CCN concentration for 60 nm particles exhibit a substantial increase.~~ This event, together with others of smaller extent, is associated with new particle formation (NFP) events. The observed frequency of NPF days at Finokalia is close to 30% (Kalivitis et al., 2015), regardless of the presence or not of BB-laden air masses. Based on aerosol chemical composition it appears that both gaseous sulfuric acid and organic compounds take part in the growth of nucleated particles to CCN-relevant sizes. These organic compounds that contribute to the nuclei growth may be of different origins including biogenic emissions, biomass burning and other possibly anthropogenic sources from long-range transport (Kalivitis et al. 2015). ~~It~~ From Figure 4b it appears that when the BB event is combined with ~~a~~ such an NPF event within a few hours, 60-nm particles are strongly influenced and their CCN concentrations increase considerably. The influence of BB to the hygroscopicity of 60-nm particles and the other sizes is examined in a subsequent section. A detailed discussion on these events and their contribution to CCN concentrations is provided by Kalivitis et al. (2015).

3.4 CCN activation fractions during fire events

As demonstrated in the preceding section, CCN number concentrations during the biomass burning events ~~CCN number concentrations of~~ proportionately increased for ~~mostly~~ the larger particle sizes. ~~augmented, and so did the total number concentrations at the corresponding particle size, with the exception of the smaller ones.~~ Figure 5 shows the activation fractions (~~CCN/CN~~$R_a(Q)$) for three of the four particle sizes and the four considered fire events~~, as once more particles of (100 and~~ 120 nm is not shown as it exhibits ~~a similar~~the same behavior as 100 nm). ~~In this case, instead of the BBOA factor, the concentration of the~~As an indicator of BB influence, we use the concentration of the aged BB factor identified in the ACSM spectra ~~processed BBOA~~ (OOA-BB), as it ~~which~~ represents the atmospherically-processed component of BBOA~~, is given for reference~~. This factor is chosen as it constitutes a larger part of the organic aerosol (30%) with BB influence and whose ageing is expected to be reflected in terms of CCN activity.

For all particle sizes, the activation fractions are derived from the asymptote of the fitting to the sigmoidal function of the $R_a(s)$ during each supersaturation cycle and represents the CCN behavior at the highest supersaturations measured (s>0.6%). Figure 5 shows that even though CCN concentrations increase for particles larger than 80 nm, ~~First of all, it can be seen that apart from the 60 nm particles, the remaining sizes appear to be unaffected by the presence of smoke, as~~ their activation fractions ~~at supersaturation levels as low as 0.4%~~ remain, more or less, stable and very close to unity throughout the events. This observation implies that~~,~~ almost all aerosol particles larger than 80 nm are CCN active at supersaturations higher than 0.6%, within uncertainties. This is not the case for 60 nm particles whose activation fractions at 0.6% s (and in the case of the Chios fire activation fractions of 80 nm particles as well at 0.4% s) exhibit the highest variability, with ratios approaching values as low as 40%. It can be seen that as concentrations of the OOA-BB start to increase, the ~~$R_a(60_{nm})$~~activation fractions of 60 nm particles at ~0.6% ~~S~~s start~~s~~ to diminish.~~In addition, larger particles tend to be internally mixed, which can justify their high $R_a(d_p)$ at the point of their characteristic supersaturation.~~ It thus appears, that larger particles are mostly internally mixed, as also seen by their high activation ratios, while small particles could be externally mixed populations. An indication of the heterogeneity of the smaller particle sizes compared to the larger ones is the slope of the sigmoid fit to the $Ra(s)$; the steeper the slope the more homogeneous the population and given that the 60 nm particles exhibited the broader slopes, the more heterogeneous these particles are. This can be explained by a size-dependent chemical composition and the presence of a population with notable lower hygroscopicity that prohibits the particles from acting as CCN and ~~This~~ can be attributed to different sources and atmospheric processing (coagulation, cloud processing and condensation of secondary aerosol) ~~components~~ that ~~are usually more hygroscopic, particles are also~~generally tend to internally mix the particles, rendering them more CCN active. Indeed, the ~~lower~~ lowest activation fractions occur for the strongest events where the time for transport and aging is most limited (hence least aged and hygroscopic). ~~This aspect is further supported by t~~The particle chemical dispersion retrievals ~~discussed in the following section~~ (Section 3.5) also supports this view. The same conclusion is also drawn from the data provided by Bougiatioti et al. (2011) for the same sampling site during summertime, and are verified by analysis of the chemical dispersion and HTDMA data shown in following sections. The evolution of the mixing state of each particle size is further investigated by the HTDMA measurements in a subsequent section (Section 3.6) as well.~~The same conclusion is also drawn from the data provided by Bougiatioti et al. (2011) for the same sampling site during summertime, and are verified by analysis of the chemical dispersion and HTDMA data shown in following sections.~~

~~In contrast to the above, $R_a(60_{nm})$ at 0.6% S (and in the case of the Chios fire $R_a(80_{nm})$ at 0.4% S) exhibits the highest variability, with ratios reaching at some cases even 40%. This indicates that a substantial fraction of the smaller particle sizes may well be an external mixture with low hygroscopicity particles that do not act as CCN up to ~0.6% supersaturation. Indeed, the lower activation fractions occur for the strongest events where the time for transport and aging is limited. This aspect is further~~

~~supported by the particle chemical dispersion retrievals discussed in the following section.~~

~~The mixing state of the different sampled particle sizes is also investigated by the HTDMA measurements (Section 3.6). For reference, the concentration of the OOA-BB factor is also provided in Figure 5, which represents an oxygenated organic aerosol which is derived from the atmospheric processing of biomass burning organic aerosol (Bougiatioti et al., 2014). It can be seen that as concentrations of the OOA-BB start to increase, the $R_a(60_{nm})$ at ~0.6% S starts to diminish. This is also the case for the Croatia fire, even though the CCN concentrations did not fluctuate much from background levels because of the longer transport. It appears, thus that larger particles are mostly internally mixed, as also seen by their high activation ratios, while small particles could be externally mixed populations. This behavior is further discussed in the following section.~~

3.5 Hygroscopicity and chemical heterogeneity during the biomass burning events

The characteristic hygroscopicity parameters, κ*, derived from the CCN measurements for all particle sizes and for the four selected fire events are presented in Figure 6. As a reference for the arrival time and magnitude of the event, the concentration of the BBOA factor is also shown in the figure, which has the characteristics of the freshly-emitted BB aerosol and is expected to influence more the hygroscopicity of the particles. The smaller particles have the lowest κ_{CCN} values, and hygroscopicity consistently increased with size. This hygroscopicity trend has also been observed elsewhere (Dusek et al., 2010; Cerully et al., 2011; Levin et al., 2012; Paramonov et al., 2013; Liu et al., 2014), and is attributed to the enrichment in organic material of sub-100 nm particles. Based on the derived κ values for each particle size and with knowledge of the distinct species identified by the ACSM (organics, sulfate) and their respective hygroscopicities, the volume fractions for organics and inorganics (mainly ammonium sulfate) were estimated for each particle size. It occurs that indeed, 60 nm particles are, on average, 89% composed of organics while the respective values for 80, 100 and 120 nm particles are 70, 50 and 41%. Most of the accumulation mode particles result from condensation of secondary sulfates, nitrates and organics from the gas phase and coagulation of smaller particles (Seinfeld and Pandis, 2006). In order to examine the contribution of constituents from primary sources that are not measured by the ACSM to the accumulation mode particles, we compared the mass derived from the ACSM+BC and the integrated volume distribution from the SMPS converted to mass. During the examined fire events, the ACSM+BC was on average 68.6±19.3% of the SMPS-derived mass. Therefore this is an indication that non-refractory material neglected by the ACSM in the accumulation mode particles bears a small influence on particle hygroscopicity. Accumulation mode particles can also result from cloud processing and based on cloud droplet calculations presented in a subsequent section (Section 3.8) it appears that particles subject to atmospheric processing would be present in a separate mode are around 120 nm (s_{max} ~ 0.08%). ~~On the other hand, particles~~ Particles larger than 100 nm are usually more aged than the smaller particles and more immediately associated with BB plumes and the

atmospheric processing they undergo (Kalivitis et al., 2015). The hygroscopicity parameter for 100 and 120 nm particles are very similar and the fact that the variability in the respective chemical composition is limited may indeed be attributed to cloud processing, while 80-nm particles are in between the lowest and highest κ_{CCN} values, an indication of size-dependent chemical composition of components with different hygroscopicities.

Figure 6 also shows that during the arrival of the biomass burning-laden air masses, κ values of all particle size ranges within 0.2-0.3. This observation is consistent with values observed from chamber experiments of fresh and aged biomass burning aerosol and in-situ studies from the field. Engelhart et al. (2012) performed a study where 12 different biomass fuels commonly burnt in North American wildfires were used to characterize their respective hygroscopicity. They found that while κ of freshly emitted BBOA prior to photochemical aging covered a range from 0.06 to 0.6, after a few hours of photochemical processing, the variability of biomass burning κ values from the different fuels was reduced and hygroscopicity converged to a value of 0.2±0.1 (Cerully et al., 2011; Engelhart et al., 2012). Based on the derived hygroscopicity parameters for each particles size before and during the BB influence it occurs that smoke causes a relative decrease of κ in the order of 22% for 80 nm particles, 30.6% for 100 nm particles and 30.9% for 120 nm particles on average for the four events while κ for 60 nm particles deviate by 14%.

During the fire events the contribution of organics and BC to the submicron aerosol mass fraction increased significantly while the presence of sulfate declined. This is expected to influence the CCN activity of the sampled aerosol particles as it would cause variations in the inorganic and organic mass fractions. It has already been established that as the organic mass fraction of aerosol increases, the κ value of primary aerosol decreases (Petters et al., 2009; Engelhart et al., 2012). With photochemical aging, the increased oxygenation of the freshly emitted BBOA may influence the hygroscopicity of the organic components, but the concurrent increase of the inorganic fraction of the aerosol contributes to the observed increase of κ_{CCN} (inorganic content vs aging).

~~In order t~~To examine the ~~role~~ impact of atmospheric processing and aging ~~to~~ on the composition of the sampled aerosol, we studied the chemical dispersion $\sigma(\kappa)$~~,~~ of the hygroscopicity parameter κ, expressed by the standard deviation of kappa around the most probable hygroscopicity κ^*, and its dependence on particle size. As normal operation uncertainties and the DMA transfer function can induce a broadening of $R_a(s)$ and $R_a(\kappa)$ and therefore contribute to $\sigma(\kappa)$, the inferred $\sigma(\kappa)$ contains a fairly constant instrument offset and a time-dependent constituent that is representative of the real chemical variability. This offset value, owing to the DMA transfer function and other instrument limits has been calculated to be roughly 0.25 ~~by~~ (Cerully et al. ~~(~~2011). Table 1 shows the calculated chemical dispersion, in terms of $\sigma(\kappa)/\kappa$, for the four fire events and the measured particle sizes. It is immediately apparent that the chemical dispersion is reduced with increasing particle size. 60-nm particles exhibit the highest dispersion ~~and~~ especially ~~the ones from~~for the Chios fire, suggesting that the smaller particles ~~retain their characteristics for a longer period and their aging takes longer that for the larger particles.~~ are a mixture of freshly-emitted BB particles and particles

formed from the condensation of organics during the transport from the fire location to Finokalia, as by atmospheric processing organics become less volatile, increasing the chemical dispersion. The 80 and 100-nm particles from the Chios fire have high $\sigma(\kappa)/\kappa$ values while the ones from Euboea and Andros have considerably lower values, demonstrating the magnitude of the Chios fire and the degree of atmospheric processing that has taken place. Finally, 120-nm particles always have a low chemical dispersion, with $\sigma(\kappa)/\kappa$ values close to the instrument limit. Nevertheless, the chemical dispersion of all particle sizes appears to be influenced by the presence of BB as there is an average relative increase of $\sigma(\kappa)/\kappa$ values of 21, 28, 41 and 43% for 60, 80, 100 and 120 nm particles, respectively, before and during the event. The increased chemical dispersion of particles smaller than 80 nm can be, therefore, attributed to the heterogeneity of sources of these particles (which is also seen by CALIOP, Figure 3c) combined with lack of extensive cloud processing because the particles are too small to activate in boundary layer clouds in the region (Section 3.8). For larger particles, the chemical dispersion may be due to mixing with other types of aerosol that are not identified by the ACSM; microphysical processing such as condensational growth and cloud processing may be the reason why they exhibit a smaller chemical dispersion than smaller particles. Indeed, the surface area distributions (Figure S1 of the Supplement) peaks at around 200 nm which means that condensation of SOA mass is most effective in that size range. Coagulation/condensation continuously occurs together with any new source and NPF during atmospheric transport (Triantafyllou et al., 2016; Kalkavouras et al., in review), but cloud processing mixes everything and makes it completely homogeneous at the activation diameter that corresponds to each fire separately. In terms of aerosol microphysical processes, numerical simulations indicate that for half a day of aging under moderately polluted conditions, coagulation has been found to internally mix almost all particles above 0.2 μm, and smaller particles to a lesser extent (e.g. Jacobson, 2002). Condensation, for the same time scale, increases the fractional coating of small particles rather than large ones. ~~This behavior of the small particles may be partially due to the coagulation of ultrafine particles which are present in biomass burning plumes, as the coagulation mostly occurs for smaller particles and increases the external mixing of those particles by bringing together particles of different nature. It is also possible that organic compounds that are emitted during biomass burning events and undergo atmospheric processing during their transport, could condense on the existing particles, contributing thus to their mass. This condensational growth tends to render particles more chemically uniform, and if this condensation takes place in the smaller particle range it would have a larger impact on their chemical composition, than for the larger ones. Both condensational growth and coagulation processes can take place, with the overall observed behavior depending on which process is predominant (Healy et al., 2014). Based on the surface area distributions (Figure S1 of the supplement) it occurred that the peak of the surface area is around 200 nm. With the surface area distribution being constant, one can argue that larger particle sizes would receive most of the condensational mass. For the Chios fire, where the peak in the number size distribution is in the smaller particle range, coagulation is more effective for the 60- and 80-nm particles. This is further supported by the elevated chemical dispersion of those sizes caused by the coagulation~~

~~and the lower chemical dispersion of 100- and 120-nm particles caused by the condensation. On the other hand, during the Euboea fire where the peak in the number size distribution is closer to the peak of the surface area distribution, it seems that mostly the 60 nm particles are subject to coagulation. Larger particles could be affected by both condensation and coagulation but the chemical dispersion as a function of particle size indicates that mostly condensation processes dominate in the BB plumes. For this reason, the hygroscopicity parameters are calculated for all events and particle sizes in the following section.~~

3.6 Particle growth factors during the fire events

From the concurrent HTDMA growth factor measurements at sub-saturated conditions we calculated the corresponding κ_{HTDMA} values. During the focus period of the biomass burning events as well as a few days before and after the events, the grand majority of the HTDMA data exhibited unimodal distributions, indicating that all selected particle fractions were internally mixed. Bimodal hygroscopicity distributions were ~~scarce~~ only observed during the arrival of the smoke plumes from the most intense events and therefore are not taken into account for ~~this specific~~the comparison study between CFSTGC and HTDMA-derived κ values. Average CFSTGC-derived κ_{CCN} values and HTDMA-derived κ_{HTDMA} values for the selected particles sizes are given in Table 2. On average, κ_{HTDMA} values are somewhat lower than the respective κ_{CCN} values for the smaller particles, while the difference between them is larger for the larger particle sizes. Nevertheless, both time series follow the same trend and values are consistent within ±30% (κ_{HTDMA}=0.854 · κ_{CCN}, R^2=0.87; Figure S2 in the supplement). Owing to non-ideality in the aqueous phase, ~~Given that the solution of the resulting droplets may be non-ideal, the constituents may be partially~~ partial solubility of the organics and the existence of multiple phases under subsaturated conditions ~~soluble and the phases may not be completely separated, it is not surprising that the~~ HTDMA-derived κ_{HTDMA} values may indeed be lower than the corresponding CCN-derived ones. ~~are somewhat lower~~. In the study of Wu et al. (2013) κ derived from CCN measurements was also roughly 30% higher than that determined from hygroscopic growth measurements. Similar effects are also seen for laboratory generated aerosol composed of single and multiple compounds (Petters and Kreidenweis, 2007). Apart from non-ideality solution effects, the presence of surfactants produced during biomass burning events (Asa-Awuku et al., 2008) may also increase the discrepancies between κ-HTDMA and κ-CCN (Ruehl et al., 2012). ~~Therefore,~~Other studies as well note similar magnitude of difference ~~these differences are well within the range of possible uncertainties and are common when comparing~~ between CFSTGC and HTDMA-derived κ values (e.g. Prenni et al., 2007; Massoli et al., 2010; Cerully et al. 2011).

The probability distribution of growth factors in the HTDMA give an independent measure of particle mixing state. ~~Apart from the hygroscopicity parameter, κ_{HTDMA}, from the concurrent HTDMA measurements the mixing state of the sampled particle sizes were also determined.~~ During the two most intense fire events (i.e. during the Chios and Euboea fire) where the smoke plume had the least amount of transit and

atmospheric processing time ~~(i.e. during the Chios and Euboea fire)~~ all sizes exhibited two different hygroscopic modes (Tables 3 and 4; Figure S3 in the supplement). These distinct modes were not observed during the ~~rest of the~~other two ~~-~~events, ~~probably due to the lower intensity of the other events and the longer transport time~~owing to longer time of processing that allows for condensation growth and mixing of the populations. Figure 7 portrays in the left-hand panels the $\overline{\kappa_{HTDMA}}$ (estimated using Equation 6) for the sampled particle sizes during the Chios and Euboea fires. The right-hand panels show the respective particle size distributions obtained by the concurrent SMPS measurements, revealing the presence of different particle modes. It should be noted that values differ from the respective κ_{CCN} values, under subsaturated conditions, because if some particles do not grow inside the HTDMA they are directly assigned with a growth factor equal to one (i.e. κ=0), subsequently reducing considerably the derived kappa value. These hydrophobic particles are likely not fully counted by the CFSTGC and hence do not contribute to the average κ_{CCN}. During the arrival of the smoke-influenced air masses, there is a decrease in the hygroscopicity of all measured sizes. At the same time a bimodal distribution was observed by the SMPS (far right panels), indicative of two groups of particles, which can be partially due to the presence ~~probably~~ freshly emitted particles (i.e. smaller mode) in combination with larger, more processed ones. Adler et al. (2011) had also observed a shift in the average mode diameter of size distributions from 86±8nm for freshly-emitted BBOA to 114±7 nm for processed BBOA. This further supports the observed higher chemical dispersion ~~found~~ in the smaller particle sizes~~, presented in the previous section.~~(Section 3.5).

A similar behavior when the sampled particles influenced by biomass burning were exposed to sub-saturated conditions has been reported by Rissler et al. (2006). In those measurements the hygroscopic growth of the sampled particles when exposed at 90% RH showed that there was an external mixture of a nearly hydrophobic ($g_{(RH)}$=1.09 for 100 nm particles) and a moderately hygroscopic ($g_{(RH)}$=1.26) population. This reinforces our observations from the CCN measurements, where ~~in~~ for super-saturated conditions, the activation fraction of mainly the 60 nm particles decreased significantly under influence of the smoke. A possible explanation why the activation fractions of the other size ranges ~~seem to be unaffected by the smoke~~remain close to unity during the smoke influence may be resulting from the cloud processing of these sizes and their mixing with background particles, contributing to their hygroscopicity and chemical dispersion. The overall characteristics are expected to be determined by the number fraction of the two modes in each size, combined with the occurrence of these two modes. If the presence of the bimodal samples is limited (less than 30%), then even though the fraction of the less hygroscopic mode may be as high as 45%, the overall activation fractions might not be influenced. For the first event (20-21/8) which was the most intense, the externally mixed samples represent almost 25% of the total sampled aerosol, with the occurrence of the bimodal samples increasing with increasing diameter (Table 3). It appears that in the bimodal samples the less hygroscopic mode initially dominates followed by a progressive dominance of the hygroscopic mode. It also appears that the increase in the less hygroscopic fraction coincides with the plume arrival time and the increase of the BBOA component, further

supporting our findings of external mixing. During the second event (03-05/9) the bimodal samples increase, once more, with increasing diameter (5% for 60 nm to 28% for 120 nm particles). ~~with the~~The less hygroscopic fraction ~~being~~ in this case was dominant in approximately 33% of the samples, although this more hygroscopic mode ~~has~~ had a κ_{HTDMA} value of 0.2 during the plume arrival time (Table 4). The more hygroscopic mode is therefore dominant in number for all sampled particles, which would explain that the activation fraction of the larger accumulation mode particles are not significantly affected by the presence of the less hygroscopic mode. On the other hand, the reason for the reduction of the activation fraction of 60-nm particles, apart from their hygroscopicity, can also be their different source and size, as during the events, the less hygroscopic mode is probably not activated, thus not detected by the CCN. This is not the case for the larger particles, as for example, 80-nm particles having a low κ_{HTDMA}=0.06 will still activate at ~~a critical~~the highest supersaturations sampled ~~of~~ (s=0.67%).

3.7 Inferring size-dependent chemical composition and organic hygroscopicity

Assuming that the total aerosol hygroscopicity can be represented as the sum of the contribution of the different aerosol components:

$$\kappa = \sum_j \varepsilon_j \kappa_j \tag{7}$$

where ε_j and κ_j are the volume fraction and hygroscopicity parameters of each species, respectively (Petters and Kreidenweis, 2007). With the use of this equation, and by assuming that the aerosol is a mixture of an organic and inorganic component, with the inorganic component being represented by ammonium sulfate, the total measured hygroscopicity, can be expressed by the sum:

$$\kappa = \varepsilon_{inorg}\kappa_{inorg} + \varepsilon_{org}\kappa_{org} \tag{8}$$

Prior studies at Finokalia (Bougiatioti et al. 2009; 2011) have determined κ_{org}=0.158 and κ_{inorg}=0.6. Assuming this still applies and $\varepsilon_{inorg}+\varepsilon_{org}$=1, Equation 8 can be used to infer the volume fractions of organics and ammonium sulfate for the 4 different sizes, excluding the days of direct biomass burning influence. From this we obtain that 60 nm particles, on average, are composed of 82% organics and 18% ammonium sulfate; 80 nm particles of 44% organics and 55% ammonium sulfate, and, the larger particles ~~are mainly composed~~contain a much larger fraction of ammonium sulfate (67% and 78% for 100 and 120 nm particles, respectively). This reinforces our conclusion based on the hygroscopicity measurements that the smaller particles are mostly composed of organic material. These observations are in agreement with similar observations reported by Bezantakos et al. (2013) in the region of the Northern Aegean Sea.

The above approach can also be applied to the data from the fire events, as follows: we use only the larger size (120 nm) as from the former CCN studies in the area it was established that the hygroscopicity of the larger particles is close to the "bulk" hygroscopicity of the sampled aerosol (PM_1), which is constrained from the ACSM measurements (Bougiatioti et al., 2011). To evaluate the importance of the assumptions made in inferring the organic hygroscopicity from chemical composition,

κ_{org} was additionally determined by applying Equation 8, for the 120 nm particles, where a set of κ equations is produced (n=228). Multivariable regression analysis within the excel environment is subsequently applied in order to determine the organic and inorganic component of the total hygroscopicity during the fire events. Based on the results, κ_{inorg}=0.61±0.03 and κ_{org}=0.137±0.02, values which are very similar to values determined by Bougiatioti et al. (2009; 2011). The confidence level is 95% and the resulting fit has an R^2=0.91 and p-values are smaller than $8 \cdot 10^{-7}$ for both components.

Taking the analysis one step further, we attempt a source apportionment of the organic hygroscopicity, by its attribution to different factors. Positive Matrix Factorization (PMF) analysis was applied to the time series of data from the direct influence from biomass burning. A detailed discussion of the PMF results can be found in Bougiatioti et al. (2014). During the focus period, 3 subtypes of organic aerosol (OA) were identified, namely biomass burning OA (BBOA), an OOA associated with biomass burning (OOA-BB) and a highly oxygenated OOA, having a relative contribution of 22, 32 and 46%, respectively. With the chemical composition measurements of the ACSM for the larger particle size (120 nm) combined with the respective κ_{CCN} we use the following equation to determine the hygroscopicity parameter of each factor:

$$\kappa = (1-\varepsilon_{org})\kappa_{inorg} + \varepsilon_{BBOA}\kappa_{BBOA} + \varepsilon_{OOA-BB}\kappa_{OOA-BB} + \varepsilon_{OOA}\kappa_{OOA} \quad (9)$$

Once again a set of 228 κ equations is produced and multivariable regression analysis is applied in order to deconvolve the organic hygroscopicity to its 3 subtypes. The confidence level once more is 95% and the resulting fit has an R^2=0.93, with p-values smaller than 0.001. It occurs that κ_{inorg}=0.62±0.04, κ_{BBOA}=0.057±0.07, κ_{OOA-BB}=0.138±0.11 and κ_{OOA}=0.169±0.09. As the occurrence of two modes of different hygroscopicity seen by the HTDMA during the arrival of the smoke coincide with the identification of BBOA by the ACSM, ~~i~~It is interesting to see that the inferred hygroscopicity for the freshly-emitted BBOA is very close to the hygroscopicity obtained by the HTDMA for the less hygroscopic component when two particle populations were present during the events (Tables 3 and 4, Section 3.6). When comparing the obtained hygroscopicity with the level of oxidation of each factor (O:C=0.2 for BBOA, 0.9 for OOA-BB and 1.2 for OOA; Bougiatioti et al., 2014) it occurs that the less hygroscopic component is also the least oxygenated and hygroscopicity increases with increasing O:C ratio. The calculated values are also comparable to the κ obtained by Chang et al. (2010) for the oxygenated organic component (OOA-1, OOA-2 and BBOA) of rural aerosol (κ_{ox}=0.22±0.04). They also found increased hygroscopicity with increasing ageing and degree of oxidation. Furthermore, the total organic hygroscopicity is very similar to ~~the hygroscopicity~~that of the processed organic aerosol components, which make up almost 80% of the organic aerosol. Finally, based on the derived hygroscopicities for the BBOA and the processed BBOA (OOA-BB), it seems that the biomass burning organic aerosol becomes more hygroscopic, by almost a factor of two, with atmospheric processing.

Using the average diurnal profiles obtained from the PMF analysis combined with the corresponding mass fractions of each component and the inferred hygroscopicity parameter of each, we estimated the contribution of each factor to the overall κ_{org} and

the total aerosol hygroscopicity. Figure 8 presents the resulting diurnal profiles ~~and~~ from which it is clear that the grand majority of the organic hygroscopicity originates from the aged, very oxidized OOA. BBOA contributes around 7% to the organic hygroscopicity (2.2% to the overall aerosol hygroscopicity), which is small but not negligible, as it can be seen that when the BBOA contribution is the highest, there is an important decrease in the κ_{org}. Overall, organic aerosol associated with biomass burning can account for almost 35% of the organic hygroscopicity. By using the approach of Guo et al. (2015) where particle water is predicted using meteorological observations (relative humidity, temperature), aerosol composition and thermodynamic modeling (ISORROPIA-II; Fountoukis and Nenes, 2007), the LWC associated with the organic fraction is calculated. ~~It occurs~~We find that ~~even though~~although the freshly-emitted BBOA contributes merely 1.2% to the total organic water of the aerosol, the ~~corresponding~~ contribution of the processed OOA-BB is almost 33%. It is therefore clear that in the presence of biomass burning aerosol, both aerosol hygroscopicity but LWC as well may be influenced, thus affecting the overall direct and indirect aerosol radiative effects.

3.8 BB influence on droplet formation

The direct microphysical link between aerosol and clouds is the activation process, where a fraction of the aerosol contained within an ascending cloud parcel experiences unconstrained growth and activates to form cloud droplets. State of the art cloud droplet parameterizations (Ghan et al., 2011; Morales and Nenes, 2014) can accurately and rapidly calculate the droplet number (N_d) and maximum supersaturation (S_{max}) that would form in a cloud given knowledge of the aerosol distribution, composition and updraft velocity. Using the aerosol and hygroscopicity observations from all four BB events, we calculate the droplet number and supersaturation for clouds forming in the vicinity of Finokalia, using the droplet parameterizations based on the "population splitting concept" of Nenes and Seinfeld (2003), later improved by Barahona et al., (2010) and Morales and Nenes (2014). In the calculations of droplet number, the size distribution is represented by the sectional approach, derived directly from the SMPS distribution files. Values of updraft velocity are not known for Finokalia, but are obtained from the WRF regional model applied to late summer conditions (Tombrou et al., 2015); simulations suggest that the distribution of vertical velocities in the boundary layer around Finokalia display a spectral dispersion of σ_w = 0.2-0.3 m s^{-1} around a mean average value of 0.3. These values are generally consistent with vertical velocities observed in marine boundary layers (e.g., Ghate et al., 2011; Meskhidze et al., 2005). Given this, we can employ the characteristic velocity approach of Morales and Nenes (2010) when applying the droplet parameterization to obtain velocity PDF-averaged values of CDNC and S_{max}. As a sensitivity test, we also consider calculations for a convective boundary layer (σ_w = 0.6 ms^{-1}). The calculation of PDF-averaged values of CDNC and S_{max} is carried out for every distribution of aerosol number and composition measured for all four biomass burning events (5-min resolution distributions from the SMPS measurements for at least two days for each event). Results of all the calculations are shown in Figure 9. As a reference, the time series of the BBOA component is also portrayed.

For all events, the arrival of the smoke plume is followed by a considerable depression in the maximum supersaturation (relative average decrease 11.9±2.7% for σ_w = 0.3 ms^{-1} and 18±5.9% for σ_w = 0.6 ms^{-1}) that develops in clouds. This is a result of the enhanced competition for water vapor during cloud droplet formation for clouds affected by biomass burning smoke. The negative feedback of aerosol on supersaturation partially mitigates the observed increases in CCN to the point where clouds are highly insensitive to the large aerosol concentration increases (Moore et al., 2013; Zamora et al., 2016). As expected, increases in the updraft velocity (σ_w = 0.6 ms^{-1}) reduces the competition of CCN for water vapor, allowing S_{max} to increase, by almost 30%. The respective perturbation of N_d from BB influences by doubling the updraft velocity increases to 54% on average (from 9.3% to 24.2% for Chios, from 8.5% to 15.2% for Croatia, from 11% to 18.8% for Euboea and from 4% to 13.8% for Andros). The low supersaturations developed in BB-influenced clouds (here, as low as 0.06%) shifts the size of particles affected by cloud processing to the largest of particles (cutoff diameters before and during the Chios intense event were on average 133 and 109 nm, respectively while during the other events were on average 154.8 and 129.3 nm, respectively). Interestingly, the notable drop in chemical dispersion in the 100-120 nm particle sizes are consistent with the notion that cloud processing would considerably enhance their degree of internal mixing.

The degree to which BB influences N_d does not depend only on the value of updraft velocity and the intensity of the BB event; it also depends on the background aerosol. This is because the background preconditions the clouds and determines the levels of supersaturation that develops prior to the arrival of the BB aerosol. Highly polluted background generally means larger insensitivity of N_d to BB. This is shown clearly in Figure 10, which presents the droplet number concentration (top panel) and cloud maximum supersaturation (bottom panel) for each fire event as a function of BB influence, expressed by the sum of BBOA and OOA-BB ACSM factors. From the figure one can clearly see that when the background levels aerosol decreases (indicated by the lower N_d and higher S_{max} at the low end of BB factor concentrations, which is characteristic of the Coatia and Chios fires), N_d responds to increases in BB, up to the point where the clouds become "saturated" with aerosol (with a supersaturation around 0.08% and below, indicated by the shaded areas in Figure 10) and are insensitive to additional increases in BB. Euboea and Andros fires already have a high background, so the cloud droplet number is relatively insensitive to BB influence.

Finally, we estimated the relative contribution of chemical composition (from κ) and aerosol number concentration to the N_d, expressed by the average of the partial derivatives of dN_d/dN_a and dN_d/dN_κ and using the following equations:

$$\sigma^2 N_d = \sigma N_a \overline{\frac{\partial N_d}{\partial N_a}} + \sigma\kappa \overline{\frac{\partial N_d}{\partial N_\kappa}} \qquad (10)$$

where σ^2 is the variance of the droplet number (Nd), σNa is the standard deviation of the total aerosol number and $\sigma\kappa$ is the standard deviation of the hygroscopicity parameter. The relative contribution of each one of the total aerosol number (εN_a) and hygroscopicity parameter ($\varepsilon\kappa$) to the droplet number is estimated by:

$$\varepsilon\kappa_{Nd} = \sigma\kappa \frac{\overline{\frac{\partial N_d}{dN_\kappa}}}{\sigma^2 N_d} \qquad (11)$$

$$\varepsilon N_{aNd} = \sigma N_a \frac{\overline{\frac{\partial N_d}{\partial N_a}}}{\sigma^2 N_d} \qquad (12)$$

The results provided in Table 5 demonstrate that there are differences between the fire events, which can be attributed to the intensity of each event and thus the resulting concentrations, and the distance from the fire, thus the mixing and dilution during transport. The highest variance in N_d was calculated for the Andros event, which exhibited the lowest variability in $N_{aerosol}$ and the lowest variance was calculated for the Chios, followed by the Croatia event, which exhibited a variability in $N_{aerosol}$ of more than 1500 particles (cm^{-3}). From the relative contribution of the total aerosol number and chemical composition to N_d it can be seen that the closest the fire event is, the largest the contribution of aerosol number to the potential CDNC. As we move further away (e.g. Chios and Croatia) and the distance increases, the influence of the chemical composition becomes increasingly important, given the decrease of concentrations and dilution during transport.

4. Summary and Conclusions

This study provides CCN concentrations, subsaturated hygroscopicity~~ and~~, mixing state of size-selected aerosol particles and their impact on cloud formation in air masses influenced by summer biomass burning (BB) events ~~during summertime over the~~in the eastern Mediterranean. The uniqueness of the dataset examined lies in nature of the fires, where smoke is mostly generated from isolated fires and subsequently transported and aged from a few hours to days before sampling. The presence of smoke in ~~For the case of~~ the most intense events ~~the presence of smoke was~~is clearly identified by CALIPSO ~~laser~~ lidar remote sensing ~~observations for the most intense event.~~and the MODIS FIRMS product, while chemical markers and backtrajectory analysis confirm the influence of BB in every event. ~~Overall, during the selected events~~During each event, the contribution of organics and BC increased significantly while the concentration of sulfates decreased. This is shown ~~also~~ to affect the hygroscopicity as well as the mixing state of the particles. The fire events had a direct influence ~~to~~ on the total particle (CN) and CCN concentrations across all sizes; ~~where especially the larger~~ particle sizes ~~(~~larger than 100 nm~~)~~ exhibited an increase in absolute number of more than 50% and up to 30% for particles in the 60-80 nm range. ~~At the same time, the activation~~The fraction~~s~~ of the smaller particles ~~(60-80 nm) at~~acting as CCN even at the highest level of measured supersaturation (~~-~~0.6% s) however went significantly below unity ~~appeared to be affected by the~~in the presence of smoke~~, with ratios being well below unity~~. ~~Based on the observations it is inferred~~This and the overall value of hygroscopicity indicate that less CCN-active organic compounds ~~that are less CCN-active,~~ are the dominant component of 60-nm

and smaller particles (up to 82% of mass), while particles larger than 100 nm ~~are mainly composed~~contain a much larger fraction of ammonium sulfate. ~~This was verified by the~~The subsaturated hygroscopicity ~~analysis~~measurements confirms this, ~~where~~ as 60-nm particles exhibited the lowest ~~hygroscopicity~~hygroscopic growth.

~~Nevertheless, d~~During the arrival of the biomass-burning-laden air masses, the average hygroscopicity parameters of all particle sizes converged to values ~~in the range of~~between 0.2-0.3, which can be attributed to different chemical composition of all particles during these events, compared to background conditions. ~~Based on~~The hygroscopicity distributions and chemical dispersion analysis ~~it occurred~~of the CCN data clearly show that smaller particles exhibit higher chemical ~~dispersion and retain their characteristics for longer~~diversity (variance in hygroscopicity equal to 0.15 κ units)~~,~~ than ~~compared to~~ larger ~~ones that appear more homogeneous~~particles (variance in hygroscopicity less than 0.1 κ units) . This ~~can be due to the fact~~ size-dependent mixing state may reflect the presence of different aerosol sources with characteristic sizes (e.g. sea-salt, pollution in addition to BB) and size-dependent chemical composition; the fact that smaller particles are less mixed than larger particles- together with that the background aerosol is composed of a large mode with a distinct chemical composition- suggests that the smaller particles are an external mixture of freshly emitted and secondarily formed particles that retain a large degree of mixing. Larger particles are further aged and subject to coagulation, condensation of secondary species and cloud processing, all of which tend to homogenize aerosol. ~~coagulation likely promotes the chemical dispersion at smaller sizes, while the condensation of organics tends to make larger particles more uniform~~. ~~Despite that~~However, ~~samples with~~ two ~~distinct~~ aerosol populations with distinct hygroscopicity were seen were seen event at the largest sizes sampled ~~, one having lower and one somewhat higher hygroscopicity, do appear~~ during the most intense fire events. Nevertheless, their occurrence is limited and the overall activation of larger particles appears to be unaffected by the presence of these two populations. ~~Overall we can conclude that 60-nm particles were mostly composed by less hygroscopic species, even when they have undergone atmospheric processing and they were internally mixed, making it more difficult for them to activate because of their size and hygroscopicity even at the highest level of supersaturation. It appears that the dominant process in this particle range is coagulation, rendering small particles less uniform, with increased chemical dispersionOn the other hand,~~In terms of cloud processing effects, the ~~larger~~ largest particles that are predicted to form droplets in clouds in the vicinity of the sampling site indeed exhibit the lowest chemical dispersion. ~~were composed of more hygroscopic species, which either condensational growth or atmospheric aging yielded an internal mixture with lower chemical dispersion.~~ This supports the assumption of external mixing for smaller particles originating from biomass burning ~~with~~ having decreased activation fractions and provides a plausible explanation of why larger particles appear, based on their activation fractions, not to be affected as far as their CCN-activity is concerned.

~~Finally, u~~Using multivariable regression analysis and the volume fractions of organics and ammonium sulfate for the different particle sizes, we inferred the hygroscopicity of the organic fraction and found it equal to 0.115±0.017, which is ~~comparable to the~~

~~value of 0.2±0.1 determined for processed biomass burning aerosol~~consistent with published values from the literature. Using the results obtained from the source apportionment of the organic fraction we were able to deconvolve the organic hygroscopicity to its 3 subtypes. The hygroscopicity of freshly-emitted BBOA was found to be around 0.06, while the hygroscopicity of atmospherically-processed BBOA and highly oxidized organic aerosol was found to be 0.14 and 0.17, respectively. The inferred hygroscopicity of each component ~~are in line with the corresponding level of~~and its oxidation ~~of each component, and the overall organic hygroscopicity is close to the hygroscopicity derived for the processed organic aerosol~~state are in line with the overall organic aerosol values observed. ~~Thus,~~From this and the trends of each factor with atmospheric age we conclude that the organic fraction of biomass burning aerosol becomes more hygroscopic with atmospheric aging. Overall, organic aerosol associated with biomass burning (freshly emitted and processed) can account for ~~almost~~ 10% of the total aerosol hygroscopicity (2.2 and 7.6% for BBOA and OOA-BB, respectively). For the observed levels of relative humidity, and amount of each organic aerosol factor, we estimate that BBOA and OOA-BB contribute anywhere between 1.2 and 32.6% of the total organic water of the aerosol.

Towards understanding the impacts of the observed BB on clouds, we study the behavior of cloud droplet formation for typical boundary layer conditions. For this, we apply a state of the art cloud droplet formation parameterization to the observations, assuming typical values of updraft velocity for marine boundary layer clouds. We find that the very high concentrations of CCN during the influence of BB events tend to promote the competition for cloud water vapor, and substantially depresses the cloud supersaturation down to very low levels (even as low as 0.06%). As a result, only the largest of particles, from 110-150nm diameter and above, can activate to form cloud droplets. This also means that droplet number becomes highly insensitive to changes in aerosol in the presence of BB; indeed clouds influenced by BB exhibit a relative decrease in maximum supersaturation by 12% while at the same time, augments the potential droplet number by 8.5%. These results also support the chemical dispersion/mixing state analysis of the CCN data, as only the largest of aerosol sizes sampled activates and is exposed to cloud processing. Based on the average sensitivity of droplet number to changes in aerosol number and composition and observed variances thereof, we attribute the relative contribution of chemical composition and total aerosol number to the variance of droplet number. We find that the distance from the source is a key parameter that governs the importance of each parameter, with the influence of the chemical composition becoming increasingly important (controlling up to 25% of the droplet number variability) with growing distance from the source. Close to sources, the exclusive majority (98% and above) of the predicted droplet number variability is attributed to aerosol number variations. Therefore, although BB burning may strongly elevate CCN numbers, the relative impacts on cloud droplet number (compared to background levels) is eventually limited by water vapor availability and depends on the aerosol levels associated with the background.~~Taking into account the fact that organic aerosol may have important contribution to the fine-particle water (Guo et al., 2015), it is estimated that the liquid water content contribution of BBOA and OOA-BB is of the order of 1.2 and 32.6% of the total organic~~

~~water of the aerosol. This has important implications to aerosol chemistry, as aerosol water can provide the medium for heterogeneous reactions, but also can contribute to the aerosol direct and indirect radiative effect.~~

Acknowledgments

The work of A. Bougiatioti, A. Papayannis, P. Kokkalis was supported by the “MACAVE” research project and the work of N. Kalivitis by the"FRONT" research project, which are implemented within the framework~~The work of AB, AP, PK was supported by the “MACAVE” research project which is implemented within the framework~~ of the action Supporting of Postdoctoral Researchers of the Operational Program Education and Lifelong Learning (action’s beneficiary: General Secretariat for Research and Technology), and is co-financed by the European Social Fund (ESF) and the Greek State. This research has also been co-financed by the European Union (European Social Fund – ESF) and Greek national funds through the Operational Program "Education and Lifelong Learning" of the National Strategic Reference Framework (NSRF) - Research Funding Program: THALES, Investing in knowledge society through the European Social Fund. The financial support by the European Community through the ACTRIS Research Infrastructure Action and Bacchus project under the 7th Framework Programme (Grant Agreements no 262254 and 603445, respectively) are gratefully acknowledged. AN acknowledges support from a Georgia Power Faculty Scholar Chair and a Cullen-Peck Faculty Fellowship.

References

Adler, G., Flores, J.M., Abo Riziq, A., Borrmann, S., and Rudich, Y.: Chemical, physical, and optical evolution of biomass burning aerosols: a case study, Atmos. Chem. Phys., 11, 1491-1503, doi:10.5194/acp-11-1491-2011, 2011.

Andreae, M. O., Rosenfeld, D., Artaxo, P., Costa, A. A., Frank, G. P., Longo, K. M., and Silva Dias, M. A. F.: Smoking rain clouds over the Amazon, Science, 303, 1337–1342, 2004.

Asa-Awuku, A., Nenes, A., Sullivan, A.P., Hennigan, C.J. and Weber, R.J.: Investigation of molar volume and surfactant characteristics of water-soluble organic compounds in biomass burning aerosol, Atmos. Chem. Phys., 8, 799-812, 2008.

~~Asa-Awuku, A., Moore, R.H., Nenes, A., Bahreini, R., Holloway, J.S., Brock, C.A., Middlebrook, A.M., Ryerson, T., Jimenez, J., DeCarlo, P., Hecobian, A., Weber, R. Stickel, R., Tanner, D.J., Huey, L.G.:Airborne Cloud Condensation Nuclei Measurements during the 2006 Texas Air Quality Study, J. Geoph. Res., 116, D11201, doi:10.1029/2010JD014874, 2010.~~

Barahona, D., West, R.E.L., Stier, P., Romakkaniemi, S., Kokkola, H., and A. Nenes: Comprehensively Accounting for the Effect of Giant CCN in Cloud Activation Parameterizations, Atmos. Chem. Phys., 10, 2467-2473, 2010.

Bezantakos, S., K. Barmpounis, M. Giamarelou, E. Bossioli, M. Tombrou, N. Mihalopoulos, K. Eleftheriadis, J. Kalogiros, J.D. Allan, A. Bacak, C.J. Percival, H. Coe and G. Biskos: Chemical Composition and Hygroscopic Properties of Aerosol Particles over the Aegean Sea, Atmos. Chem. Phys., 13 (22), 11595–608, doi:10.5194/acp-13-11595-2013, 2013.

Biskos, G., D. Paulsen, L. M. Russell, P. R. Buseck, and S. T. Martin: Prompt Deliquescence and Efflorescence of Aerosol Nanoparticles, Atmos. Chem. Phys. 6, 4633–42, 2006.

Bougiatioti, A., Fountoukis, C., Kalivitis, N., Pandis, S.N., Nenes, A., and Mihalopoulos, N.: Cloud condensation nuclei measurements in the marine boundary layer of the eastern Mediterranean: CCN closure and droplet growth kinetics, Atmos. Chem. Phys., 9, 7053-7066, 2009.

Bougiatioti, A., Nenes, A., Fountoukis, C., Kalivitis, N., Pandis, S.N., and Mihalopoulos, N.: Size-resolved CCN distributions and activation kinetics of aged continental and marine aerosol, Atmos. Chem. Phys., 11, 8791-8808, doi:10.5194/acp-11-8791-2011, 2011.

Bougiatioti, A., Stavroulas, I., Kostenidou, E., Zarmpas, P., Theodosi, C., Kouvarakis, G., Canonaco, F., Prévôt, A.S.H., Nenes, A., Pandis, S.N., and Mihalopoulos, N.: Processing of biomass-burning aerosol in the eastern Mediterranean during summertime, Atmos. Chem. Phys., 14, 4793-4807, doi:10.5194/acp-14-4793-2014, 2014.

Carlton, A. G. and Turpin, B. J.: Particle partitioning potential of organic compounds is highest in the Eastern US and driven by anthropogenic water, Atmos. Chem. Phys., 13, 10203–10214, doi:10.5194/acp-13-10203-2013, 2013.

Cerully, K.M., Raatikainen, T., Lance, S., Tkacik, D., Tiitta, D., Petäjä, T., Ehn, M., Kulmala, M., Wornsop, D.R., Laaksonen, A., Smith, J.N. and Nenes, A.: Aerosol hygroscopicity and CCN activation kinetics in a boreal forest environment during the 2007 EUCAARI campaign, Atmos. Chem. Phys., 11, 12369-112386, doi:10.5194/acp-11-12369-2011, 2011.

Cerully, K. M., Bougiatioti, A., Hite Jr., J. R., Guo, H., Xu, L., Ng, N. L., Weber, R., and Nenes, A.: On the link between hygroscopicity, volatility, and oxidation state of ambient and water-soluble aerosol in the Southeastern United States, Atmos. Chem. Phys. Discuss., 14, 30835-30877, doi:10.5194/acpd-14-30835-2014, 2014.

Chang, R. Y-W., Slowik, J. G., Shantz, N. C., Vlasenko, A., Liggio, J.,Sjostedt, S. J., Leaitch, W. R., and Abbatt, J. P. D.: The hygroscopicity parameter (κ) of ambient organic aerosol at a field site subject to biogenic and anthropogenic influences: relationship to degree of aerosol oxidation, Atmos. Chem. Phys., 10, 5047–5064, doi:10.5194/acp-10-5047-2010, 2010.

Dusek, U., Frank, G. P., Curtius, J., Drewnick, F., Schneider, J., Kürten, A., Rose, D., Andreae, M. O., Borrmann, S., and Pöschl, U.: Enhanced organic mass fraction and decreased

hygroscopicity of cloud condensation nuclei (CCN) during NPF events, Geophys. Res. Lett., 37, L03804, doi:10.1029/2009GL040930, 2010.

Engelhart, G. J., Hennigan, C. J., Miracolo, M. A., Robinson, A. L., and Pandis, S. N.: Cloud condensation nuclei activity of fresh primary and aged biomass burning aerosol, Atmos. Chem. Phys., 12, 7285-7293, doi:10.5194/acp-12-7285-2012, 2012.

Fountoukis, C. and Nenes, A.: ISORROPIA II: a computationally efficient thermodynamic equilibrium model for K^+-Ca^{2+}-Mg^{2+}-NH_4^+-SO_4^{2-}-NO_3^--Cl^--H2O aerosols, Atmos. Chem. Phys., 7, 4639–4659, doi:10.5194/acp-7-4639-2007, 2007.

Fountoukis, C. and A. Nenes, A.: Continued Development of a Cloud Droplet Formation Parameterization for Global Climate Models, J.Geoph.Res.,110,D11212, doi:10.1029/2004JD005591, 2005.

Ghan, S.J., Abdul-Razzak, H., Nenes, A., Ming, Y., Liu, X., Ovchinnikov, M., Shipway, B., Meskhidze, N., Xu, J., Shi, X.: Droplet Nucleation: Physically-based Parameterization and Comparative Evaluation, J. Adv. Model. Earth Syst., 3, doi:10.1029/2011MS000074, 2011.

Ghate, V.P., Miller, M.A., and DiPretore, L.: Vertical velocity structure of marine boundary layer trade wind cumulus clouds, J. Geophys. Res., 116, D16, 2156-2202, doi:10.1029/2010JD015344, 2011.

Guo, H., Xu, L., Bougiatioti, A., Cerully, K.M., Capps, S.L., Hite, J.R.Jr., Carlton, A.G., Lee, S.-H., Bergin, M.H., Ng, N.L., Nenes, A., and Weber, R.J.: Fine-particle water and pH in the southeastern United States, Atmos. Chem. Phys., 15, 5211-5228, doi:10.5194/acp-15-5211-2015, 2015.

Healy, R.M., Riemer, N., Wenger, J.C., Murphy, M., West, M., Poulain, L., Wiedensohler, A., O'Connor, I.P., McGillicuddy, E., Sodeau, J.R., and Evans, G.E.: Single particle siversity and mixing state measurements, Atmos. Chem. Phys., 14, 6289-6299, doi:10.5194/acp-14-6289-2014, 2014.

Hildebrandt, L., Engelhart, G. J., Mohr, C., Kostenidou, E., Lanz, V. A., Bougiatioti, A., DeCarlo, P. F., Prevot, A. S. H., Baltensperger, U., Mihalopoulos, N., Donahue, N. M., and Pandis, S. N.: Aged organic aerosol in the Eastern Mediterranean: the Finokalia Aerosol Measurement Experiment – 2008, Atmos. Chem. Phys., 10, 4167 4186, doi:10.5194/acp-10-4167-2010, 2010.

Jacobson, M.Z.: Analysis of aerosol interactions with numerical techniques for solving coagulation, nucleation, condensation, dissolution, and reversible chemistry among multiple size distributions, J. Geophys. Res. Atmospheres, 107, D19, AAC 2-1-AAC 2-23, 2002.

Kalivitis, N., Gerasopoulos, E., Vrekoussis, M., Kouvarakis, G., Kubilay, N., Hatzianastassiou, N., Vardavas, I., and Mihalopoulos, N.: Dust transport over the eastern Mediterranean derived from Total Ozone Mapping Spectrometer, Aerosol Robotic Network, and surface measurements, J. Geophys. Res.-Atmos., 112, D03202, doi:10.1029/2006JD007510, 2007.

Kalivitis, N., Kerminen, V.-M., Kouvarakis, G., Stavroulas, I., Bougiatioti, A., Nenes, A., Manninen, H.E., Petäjä, T., Kulmala, M., and Mihalopoulos, N.: Atmospheric new particle formation as source of CCN in the Eastern Mediterranean marine boundary layer, Atmos. Chem. Phys. Discuss., 15, 11143-11178, doi:10.5194/acpd-15-11143-2015, 2015.

Kalkavouras, P., Bossioli, E., Bezantakos, S., Bougiatioti, A., Kalivitis, N., Stavroulas, I., Kouvarakis, G., Protonotariou, A.P., Dandou, A., Biskos, G., Nenes, A., Mihalopoulos, N., and Tombrou, M.: Regional variability of gaseous and particulate species and impacts on cloud formations at the South Aegean Sea during the Etesians, to be submitted to Atmos. Chem. Phys.

Kaufman, Y.J., and Remer, L.A.: Detection of forests using MID-IR reflectance-An application for aerosol studies, IEEE Trans. Geosci. Remote Sensing, 32 (3), 672-683, 1994.

Knutson, E.O., and Whitby, K.T.: Aerosol classification by electric mobility: Apparatus, theory, and applications, J. Aerosol Sci., 6, 443-451, 1975.

Kyzirakos, K., M. Karpathiotakis, G. Garbis, C. Nikolaou, K. Bereta, I. Papoutsis, T. Herekakis, D. Michail, M. Koubarakis, C. Kontoes, Wild fire monitoring using satellite images, ontologies and linked geospatial data, Web Semantics: Science, Services and Agents on the World Wide Web, 24, 18-26, 2014.

Lance, S.: Quantifying compositional impacts of ambient aerosol on cloud droplet formation, Published Doctoral Thesis, Available at http://etd.gatech.edu/theses/available/etd-11132007 175217/unrestricted/lance_sara_m_200712_phd[1].pdf, 2007.

Lance, S., Raatikainen, T., Onasch, T., Worsnop, D. R., Yu, X.-Y., Alexander, M. L., Stolzenburg, M. R., McMurry, P. H., Smith, J. N., and A. Nenes: Aerosol mixing-state, hygroscopic growth and cloud activation efficiency during MIRAGE 2006, Atmos. Chem. Phys., 13, 5049–5062, 2013.

Levin, E. J. T., Prenni, A. J., Petters, M. D., Kreidenweis, S. M., Sullivan, R. C., Atwood, S. A., Ortega, J., DeMott, P. J., and Smith, J. N.: An annual cycle of size-resolved aerosol hygroscopicity at a forested site in Colorado, J. Geophys. Res., 117, D06201, doi:10.1029/2011JD016854, 2012.

Liu, H. J., Zhao, C. S., Nekat, B., Ma, N., Wiedensohler, A., van Pinxteren, D., Spindler, G., Müller, K., and Herrmann, H.: Aerosol hygroscopicity derived from size-segregated chemical composition and its parameterization in the North China Plain, Atmos. Chem. Phys., 14, 2525–2539, doi:10.5194/acp-14-2525-2014, 2014.

Mamouri, R.E., V. Amiridis, A. Papayannis, E. Giannakaki, G. Tsaknakis, and D.S. Balis, Validation of CALIPSO space-borne derived aerosol vertical structures using a ground-based lidar in Athens, Greece, Atmos. Meas. Techn., 2, 513-522, 2009.

Mamouri, R.E., Papayannis, A., Amiridis, V., Müller, V., Kokkalis, P., Rapsomanikis, S., Karageorgos, E. T., Tsaknakis, G., Nenes, A., Kazadzis S., and Remoundaki, E.: Multi-wavelength Raman lidar, sunphotometric and aircraft measurements in combination with inversion models for the estimation of the aerosol optical and physico-chemical properties over Athens, Greece, Atmos. Meas. Tech., 5, 1793-1808, doi:10.5194/amt-5-1793-2012, 2012.

Massoli, P., Lambe, A. T., Ahern, A. T., Williams, L. R., Ehn, M., Mikkilä, J., Canagaratna, M.R., Brune, W. H., Onasch, T. B., Jayne, J. T., Petäjä, T., Kulmala, M., Laaksonen, A., Kolb, C.E., Davidovits, 5 P., and Worsnop, D. R.: Relationship between aerosol oxidation level and hygroscopic properties of laboratory generated secondary organic aerosol (SOA) particles, Geophys. Res. Lett., 37, L24801, doi:10.1029/2010GL045258, 2010.

Meskhidze, N., A. Nenes, Conant, W. C., and Seinfeld, J.H.: Evaluation of a new Cloud Droplet Activation Parameterization with In Situ Data from CRYSTAL-FACE and CSTRIPE, J. Geoph. Res., 110, D16202, doi:10.1029/2004JD005703, 2005.

Mihalopoulos, N., Stephanou, E., Kanakidou, M., Pilitsidis, S., and Bousquet, P.: Tropospheric aerosol ionic composition above the Eastern Mediterranean area, *Tellus*, **49B**, 314-326, 1997.

Moore, R.H. and Nenes, A.: Scanning Flow CCN Analysis - A Method for Fast Measurements of CCN Spectra, Aer.Sci.Tech., 43, 1192-1207, 2009.

Moore, R.H., Cerully, K., Bahreini, R., Brock, C.A., Middelbrook, A.M., and Nenes, A.: Hygroscopicity and composition of California CCN during summer 2010, J. Geophys. Res., 117, D00V12, doi:10.1029/2011JD017352, 2012a.

Moore, R.H., Raatikainen, T., Langridge, J.M., Bahreini, R., Brock, C.A., Holloway, J.S., Lack, D.A., Middlebrook, A.M., Perring, A.E., Schwarz, J.P., Spackman, J.R., and Nenes, A.: CCN spectra, hygroscopicity, and droplet activation kinetics of Secondary Organic Aerosol resulting from the 2010 Deepwater Horizon oil spill, Environ. Sci. Technol., 46, 3093-3100, 2012b.

Moore, R.H., Karydis, V.L., Capps, S.L., Lathem, T.L. and Nenes, A.: Droplet Number Prediction Uncertainties From CCN: An Integrated Assessment Using Observations and a Global Model Adjoint, Atmos. Chem. Phys., 13, 4235–4251, 2013.

Morales, R., and Nenes, A.: Characteristic updrafts for computing distribution-averaged cloud droplet number, autoconversion rate effective radius, J. Geophys. Res., 115, D18220, doi:10.1029/2009JD013233, 2010.

Morales Betancourt, R., and Nenes, A.: Aerosol Activation Parameterization: The population splitting concept revisited, Geosci. Mod. Dev., 7, 2345–2357, 2014.

Nenes, A. and Seinfeld, J.H.: Parameterization of cloud droplet formation in global climate models J.Geoph.Res, 108 (D7), 4415, doi: 10.1029/2002JD002911, 2003.

Ng, N. L., Herndon, S. C., Trimborn, A., Canagaratna, M. R., Croteau, P. L., Onasch, T. B., Sueper, D., Worsnop, D. R., Zhang, Q., Sun, Y. L., and Jayne, J. T.: An Aerosol Chemical Speciation Monitor (ACSM) for routine monitoring of the composition and mass concentration of ambient aerosol., Aerosol Sci. Tech., 45, 780–794, 2011.

Nguyen, T. B., Coggon, M. M., Flagan, R. C., and Seinfeld, J. H.: Reactive uptake and photo-Fenton oxidation of glycolaldehyde in aerosol liquid water, Environ. Sci. Technol., 47, 4307–4316, doi:10.1021/es400538j, 2013.

Omar, A. H., Winker, D. M., Kittaka, C., Vaughan, M. A., Liu, Z. Y., Hu, Y. X., Trepte, C. R., Rogers, R. R., Ferrare, R. A., Lee, K. P., Kuehn, R. E., and Hostetler, C. A.: The CALIPSO automated aerosol classification and lidar ratio selection algorithm, J. Atmos. Ocean. Tech., 26, 1994–2014, doi:10.1175/2009jtecha1231.1, 2009.

Paramonov M., P. P. Aalto, A. Asmi, N. Prisle, V.-M. Kerminen, M. Kulmala, and T. Petäjä, The analysis of size-segregated cloud condensation nuclei counter (CCNC) data and its implications for cloud droplet activation, Atmos. Chem. Phys., 13, 10285−10301, doi:10.5194/acp-13-10285-2013, 2013.

Petters, M.D., and Kreidenweis, S.M.: A single parameter representation of hygroscopic growth and cloud condensation nucleus activity, Atmos. Chem. Phys., 7, 1961-1971, doi: 10.5194/acp-8-6273-2008, 2007.

Petters, M.D., Wex, H., Carrico, C.M., Hallbauer, E., Massling, A., McMeeking, G.R., Poulain, L., Wu, Z., Kreidenweis, S.M., and Stratmann, F.: Towards closing the gap between hygroscopic growth and activation for secondary organic aerosol-Part 2: Theoretical approaches, Atmos. Chem. Phys., 9, 3999-4009, 2009.

Prenni, A.J., Petters, M.D., Kreidenweis, S.M., DeMott, P.J., and Ziemann, P.J.: Cloud droplet activation of secondary organic aerosol, J. Geophys. Res., 112, D10223, doi:10.1029/2006JD007963, 2007.

Rader, D.J., and McMurry P.H.: Application of the tandem differential mobility analyzer to studies of droplet growth or evaporation, J. Aerosol Sci., 17, 771-787, 1986.

Remy, S. and Kaiser, J. W.: Daily global fire radiative power fields estimation from one or two MODIS instruments, Atmos. Chem. Phys., 14, 13377-13390, doi:10.5194/acp-14-13377-2014, 2014.

Rissler, J., Vestin, A., Swietlicki, E., Fisch, G., Zhou, J., Artaxo, P., and Andreae, M.O.: Size distribution and hygroscopic properties of aerosol particles from dry-season biomass burning in Amazonia, Atmos. Chem. Phys., 6, 471-491, 2006.

Roberts, G., Nenes, A., Andreae, M.O., Seinfeld, J.H. (2003) Impact of Biomass Burning on Cloud Properties in the Amazon Basin, *J. Geophys. Res.*, **108**, doi: 10.1029/2001JD000985

Roberts, G.C., and Nenes, A.: A continuous-flow streamwise thermal-gradient CCN chamber for atmospheric measurements, Aerosol Sci. Technol., 39, 206-221, doi:10.1080/027868290913988, 2005.

Rose, D., Nowak, A., Achtert, P., Wiedensohler, A., Hu, M., Shao, M., Zhang, Y., Andreae, M. O., Poeschl, U.: Cloud condensation nuclei in polluted air and biomass burning smoke near

the mega-city Guangzhou, China – Part 1: Size-resolved measurements and implications for the modeling of aerosol particle hygroscopicity and CCN activity, Atmos. Chem. Phys., 10, 3365–3383, doi:10.5194/acp-10-3365-2010, 2010.

Ruehl, C., Chuang, P.Y., Nenes, A., Cappa, C., and Kolesar, K.: New Evidence of Surface Tension Reduction in Microscopic Aqueous Droplets, Geoph. Res. Let., 39, L23801, doi:10.1029/2012GL053706, 2012.

Sandradewi, J., Prevot, A. S. H., Szidat, S., Perron, N., Lanz, V. A., Weingartner, E., and Baltensperger, U.: Using aerosol light absorption measurements for the quantitative determination of wood burning and traffic emission contributions to particulate matter, Environ. Sci. Technol., 42, 3316–3323, 2008.

Sciare, J., Bardouki, H., Moulin, C., Mihalopoulos, N.: Aerosol sources and their contribution to the chemical composition of aerosols in the Eastern Mediterranean Sea during summertime, Atmos. Chem. Phys., 3, 291–302, doi:10.5194/acp-3-291-2003, 2003.

Sciare, J., Oikonomou, K., Favez, O., Liakakou, E., Markaki, Z., Cachier, H., and Mihalopoulos, N.: Long-term measurements of carbonaceous aerosols in the Eastern Mediterranean: evidence of long-range transport of biomass burning, Atmos. Chem. Phys., 8, 5551-5563, 2008.

Seinfeld, J.H., and Pandis, S.N.: Atmospheric Chemistry and Physics: From Air Pollution to Climate Change, 2nd edition, J. Wiley, New York, 2006.

Spracklen, D.V., Carslaw, K.S., Pöschl, U., Rap, A., and Forster, P.M.: Global cloud condensation nuclei influenced by carbonaceous combustion aerosol, Atmos. Chem. Phys., 11, 9067-9087, doi:10.5194/acp-11-9067-2011, 2011.

Stolzenburg, M.R., and McMurry, P.H.: TDMAFIT User's Manual, Particle Technology Laboratory, Department of Mechanical Engineering, U of Minnesota, Minneapolis, MN 55455, 1988.

Stolzenburg, M.R. and McMurry, P.H.: An ultrafine aerosol Condensation Nucleus Counter, Aerosol Sci. Technol., 14, 48-65, 1991.

Tombrou, M., Bossioli, E., Kalogiros, J., Allan, J. D., Bacak, A., Biskos, G., Coe, H., Dandou, A., Kouvarakis, G., Mihalopoulos, N., Percival, C. J., Protonotariou, A. P. and Szabó-Takács, B.: Physical and chemical processes of air masses in the Aegean Sea during Etesians: Aegean-GAME airborne campaign, Sci. Total Environ., 506-507, 201–216, doi:10.1016/j.scitotenv.2014.10.098, 2015.

Triantafyllou, E., M. Giamarelou, E. Bossioli, P. Zarmpas, C. Theodosi, C. Matsoukas, M. Tombrou, N. Mihalopoulos, and G. Biskos: Particulate Pollution Transport Episodes from Eurasia to a Remote Region of Northeast Mediterranean, Atmos. Environ., 128, 45–52, doi:10.1016/j.atmosenv.2015.12.054, 2016.

Wiedensohler, A., Birmili, W., Nowak, A., Sonntag, A., Weinhold, K. et al.: Mobility particle size spectrometers: harmonization of technical standards and data structure to facilitate high quality long-term observations of atmospheric particle number size distributions, Atmos. Meas. Tech., 5, 657-685, 2012.

Winker, D. M., Vaughan, M. A., Omar, A., Hu, Y., Powell, K. A., Liu, Z., Hunt, W. H., and Young, S. A.: Overview of the CALIPSO mission and CALIOP data processing algorithms, J. Atmos. Ocean. Tech., 26, 2310–2323, doi:10.1175/2009JTECHA1281.1, 2009.

Zamora, L.M., Kahn, R.A., Anderson, B.E., Apel, E., Diskin, G.S., Jimenez, J.L., McFarquhar, G.M., Nenes, A., Wisthaler, A., Kondo, Y., Zelenyuk-Imre, A., and Ziemba, L.: Aircraft-measured indirect cloud effects from biomass burning smoke in the Arctic and subarctic, Atmos.Chem.Phys., 16, 715-738, 2016.

Table and Figure Captions

Table 1: Calculated chemical dispersion in terms of σ(κ)/κ for the four studied fire events and all measured particle sizes.

Table 2: Average CFSTGC-derived κ_{CCN} values and HTDMA-derived κ_{HTDMA} values for the selected particles sizes.

Table 3: Percentage of externally mixed samples (B_f), the hygroscopic parameter of the less and more hygroscopic mode (κ_1, κ_2), respectively, and the number fraction of particles residing in the less hygroscopic mode (N_{f1}) during the Chios event (20-21/08/2012).

Table 4: Same as Table 3, during the Euboea event (03-05/09/2012).

Table 5: Variance of N_d and relative contribution of aerosol number and chemical composition for the four fire events.

Figure 1: Schematic of the setup used for the CCN and mixing state measurements.

Figure 2: (a) Satellite composite view from MODIS of the fire plume emerging from the island of Chios on 18 August 2012 (courtesy on NASA). The blue and red lines delineate the two ground tracks of the CALIPSO satellite during its overpass over Crete on 19 August 2012 between 00:27-00:40 and 11:34-11:47 UTC, (b) Vertical profiles of the aerosol backscatter coefficient (in $km^{-1}sr^{-1}$) at 532 and 1064 nm (left) and linear particle depolarization ratio at 532 nm (right) measured by CALIPSO and (c) Vertical profiles of the aerosol subtypes captured by CALIPSO during its overpass over Crete; the marked area is located just at the NW of Finokalia station (00:27-00:40 UTC).

Figure 3: Time series concentrations of major PM_1 species that contribute in the identification of the BB events. The shaded areas represent the four considered fire events.

Figure 4: CCN concentrations for the selected particle sizes during the arrival of the smoke plumes for (a) Chios, (b) Croatia, (c) Euboea and (d) Andros. The black solid line represents the biomass burning component of the organic aerosol at the given time.

Figure 5: Activation fractions for the selected particle sizes during the arrival of the smoke plumes for (a) Chios, (b) Croatia, (c) Euboea and (d) Andros. The brown solid line represents the processed biomass burning component of the organic aerosol.

Figure 6: Characteristic hygroscopicity parameters of the selected particle sizes for (a) Chios, (b) Croatia, (c) Euboea and (d) Andros. The solid line represents the biomass burning component of the organic aerosol at the given time and circles represent the

smoke plume arrival time. The shaded areas represent the smoke plume influence period.

Figure 7: ~~Cumulative growth factors~~Hygroscopicity parameters derived from the HTDMA (a) & (c) and number size distributions from the SMPS (b) & (d) for the Chios and Euboea fire events, respectively. The shaded areas represent the smoke plume influence period.

Figure 8: Average diurnal contribution of each organic aerosol factor to the κ_{org} computed by multiplying the mass fraction by the corresponding inferred hygroscopicity parameter and the predicted diurnal profile of the total κ_{org} in the ambient aerosol.

Figure 9: Maximum supersaturation (S_{max}) (left panels) and potential droplet number (N_d) (right panels) for the four fire events of Chios (a,b), Croatia (c,d), Euboea (e,f) and Andros (g,h).

Figure 10: Droplet number concentration (top panel) and cloud maximum supersaturation (bottom panel) for each fire event as a function of BB influence, expressed by the sum of BBOA and OOA-BB ACSM factors.

Table 1

	60 nm	*80 nm*	*100 nm*	*120 nm*
Chios	0.85±0.14	0.73±0.14	0.60±0.20	0.41±0.16
Croatia	0.77±0.18	0.68±0.19	0.44±0.12	0.41±0.10
Euboea	0.70±0.20	0.49±0.10	0.32±0.08	0.29±0.06
Andros	0.71±0.10	0.52±0.13	0.34±0.10	0.30±0.06

Table 2

	κ_{HTDMA}	κ_{CCN}
60 nm	0.23±0.07	0.22±0.05
80 nm	0.28±0.1	0.39±0.1
100 nm	0.3±0.1	0.44±0.1
120 nm	0.33±0.11	0.49±0.13

Table 3

d_p (nm)	Bf (%)	κ_1	Nf_1	κ_2
60	6.9	0.05±0.02	0.17±0.06	0.18±0.01
80	20.0	0.05±0.02	0.33±0.14	0.19±0.03
100	23.0	0.06±0.03	0.43±0.24	0.21±0.04
120	30.4	0.05±0.03	0.47±0.19	0.2±0.04

Table 4

d_p (nm)	Bf (%)	κ_1	Nf_1	κ_2
60	5.3	0.09±0.07	0.37±0.34	0.31±0.19
80	15.2	0.06±0.04	0.31±0.17	0.2±0.03
100	26.5	0.05±0.03	0.39±0.19	0.19±0.03
120	28.2	0.05±0.03	0.40±0.19	0.19±0.03

Table 5

	VarianceN_d		*Contribution_κ*		*Contribution_$N_{aerosol}$*	
	w=0.3	*w=0.6*	*w=0.3*	*w=0.6*	*w=0.3*	*w=0.6*
Chios	13.8	18.1	17.7%	12.6%	82.3%	87.4%
Croatia	34.4	47.7	26.7%	25.2%	73.3%	74.8%
Euboea	60.9	111.3	1.1%	2.2%	98.9%	97.8%
Andros	164.2	307.8	0.1%	0.15%	99.9%	99.8%

Figure 1

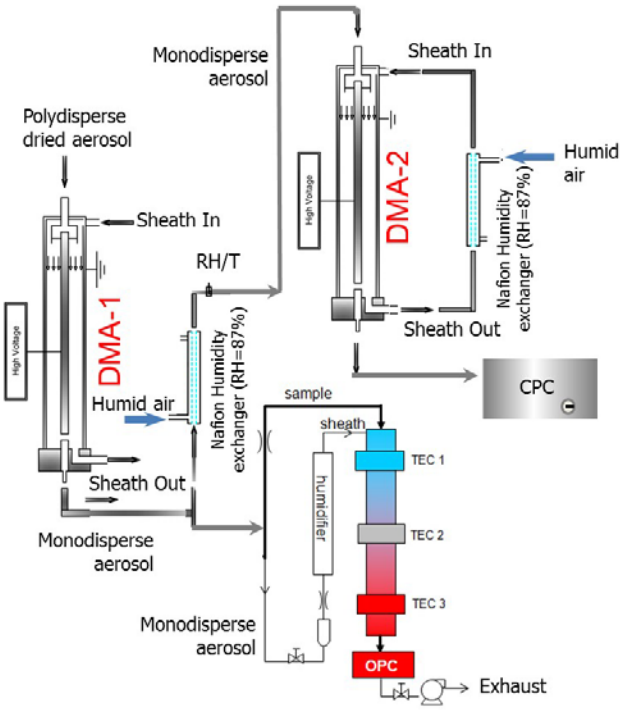
Monodisperse aerosol
Sheath In
Polydisperse dried aerosol
Humid air
DMA-2
High Voltage
Nafion Humidity exchanger (RH=87%)
Sheath In
RH/T
DMA-1
High Voltage
Sheath Out
CPC
Humid air
Nafion Humidity exchanger (RH=87%)
sample
sheath
TEC 1
humidifier
Sheath Out
TEC 2
Monodisperse aerosol
TEC 3
Monodisperse aerosol
OPC
Exhaust

Figure 2

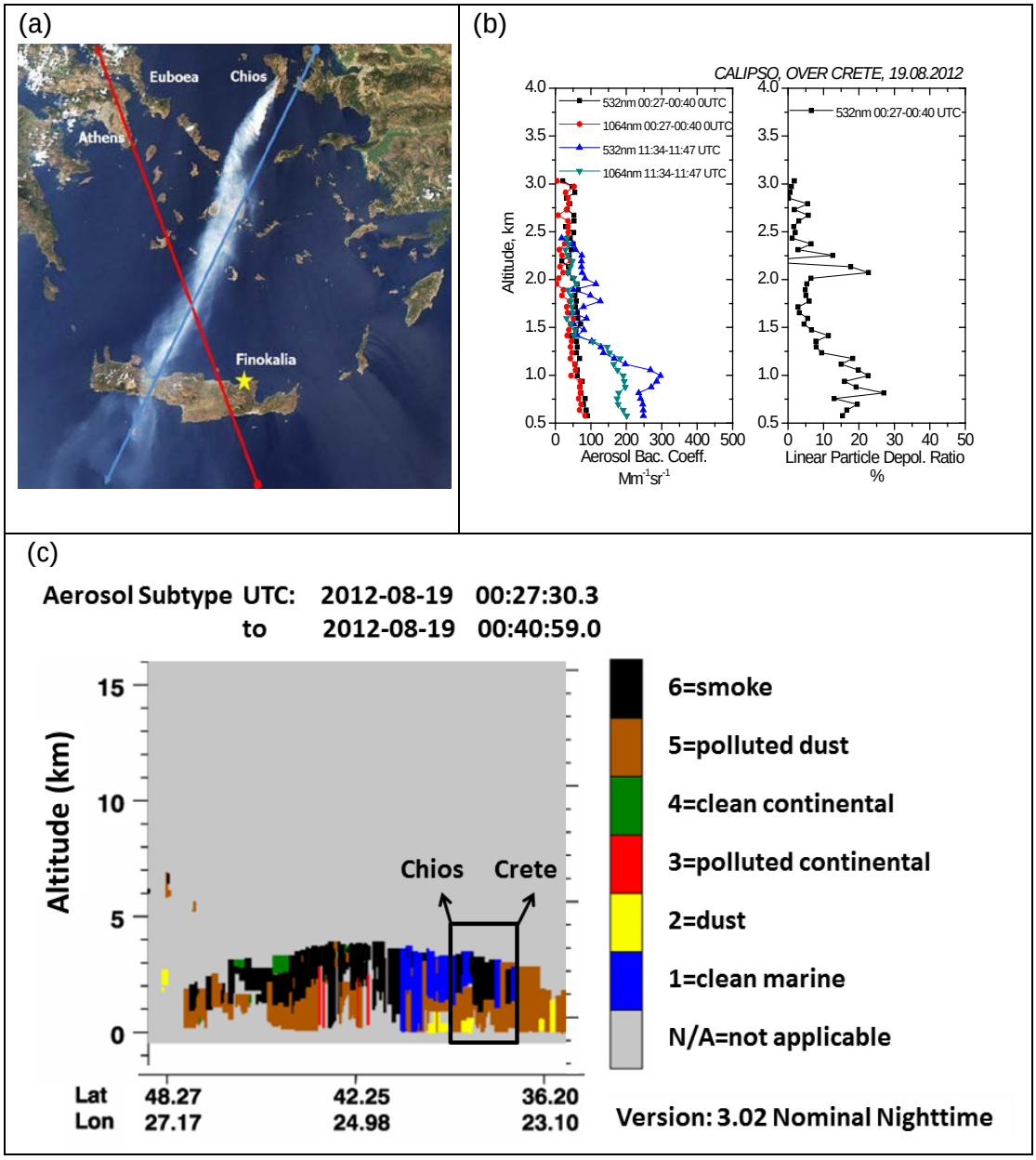
(a)
Euboea
Chios
Athens
Finokalia
(b)
CALIPSO, OVER CRETE, 19.08.2012
532nm 00:27-00:40 0UTC
1064nm 00:27-00:40 0UTC
532nm 11:34-11:47 UTC
1064nm 11:34-11:47 UTC
Altitude, km
Aerosol Bac. Coeff.
Mm-1sr-1
532nm 00:27-00:40 UTC
Linear Particle Depol. Ratio
%
(c)
Aerosol Subtype UTC: 2012-08-19 00:27:30.3
to 2012-08-19 00:40:59.0
Altitude (km)
Chios
Crete
Lat 48.27 42.25 36.20
Lon 27.17 24.98 23.10
6=smoke
5=polluted dust
4=clean continental
3=polluted continental
2=dust
1=clean marine
N/A=not applicable
Version: 3.02 Nominal Nighttime

Figure 3

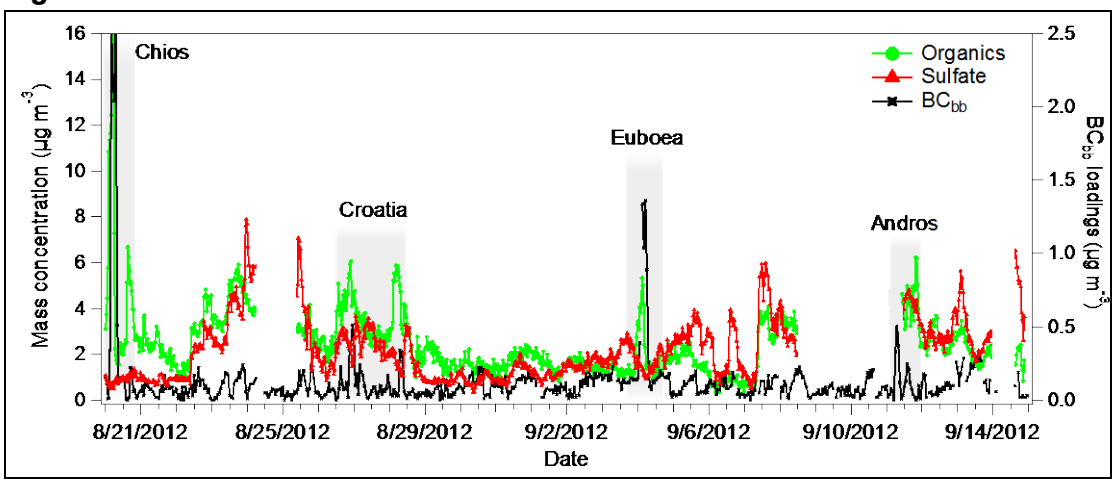
Chios
Croatia
Euboea
Andros
Organics
Sulfate
BCbb
Mass concentration (µg m-3)
BCbb loadings (µg m-3)
Date
8/21/2012
8/25/2012
8/29/2012
9/2/2012
9/6/2012
9/10/2012
9/14/2012

Figure 4

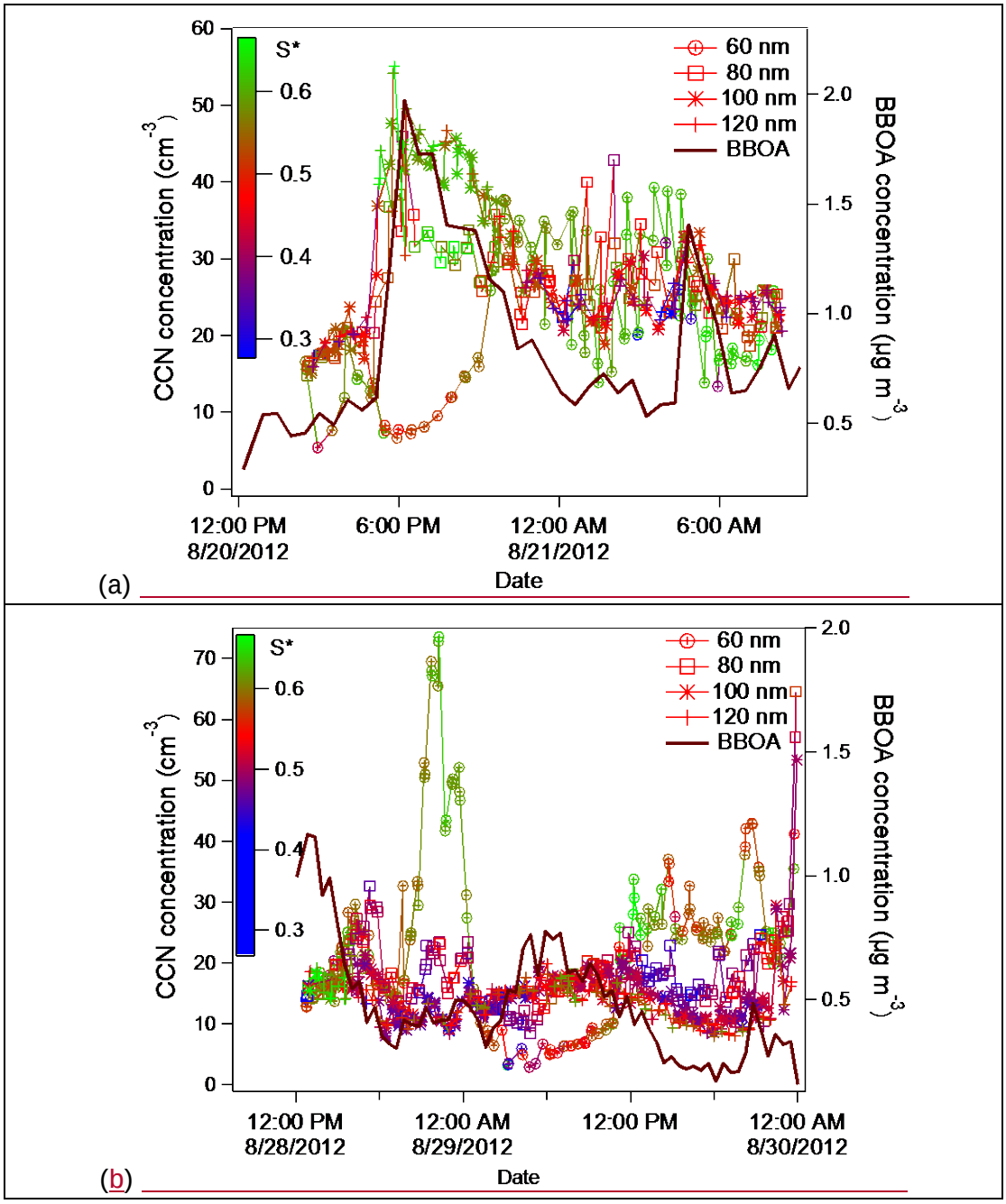
S*
0.6
0.5
0.4
0.3
60 nm
80 nm
100 nm
120 nm
BBOA
CCN concentration (cm^{-3})
BBOA concentration (μg m^{-3})
12:00 PM 8/20/2012
6:00 PM
12:00 AM 8/21/2012
6:00 AM
Date
(a)
12:00 PM 8/28/2012
12:00 AM 8/29/2012
12:00 PM
12:00 AM 8/30/2012
(b)

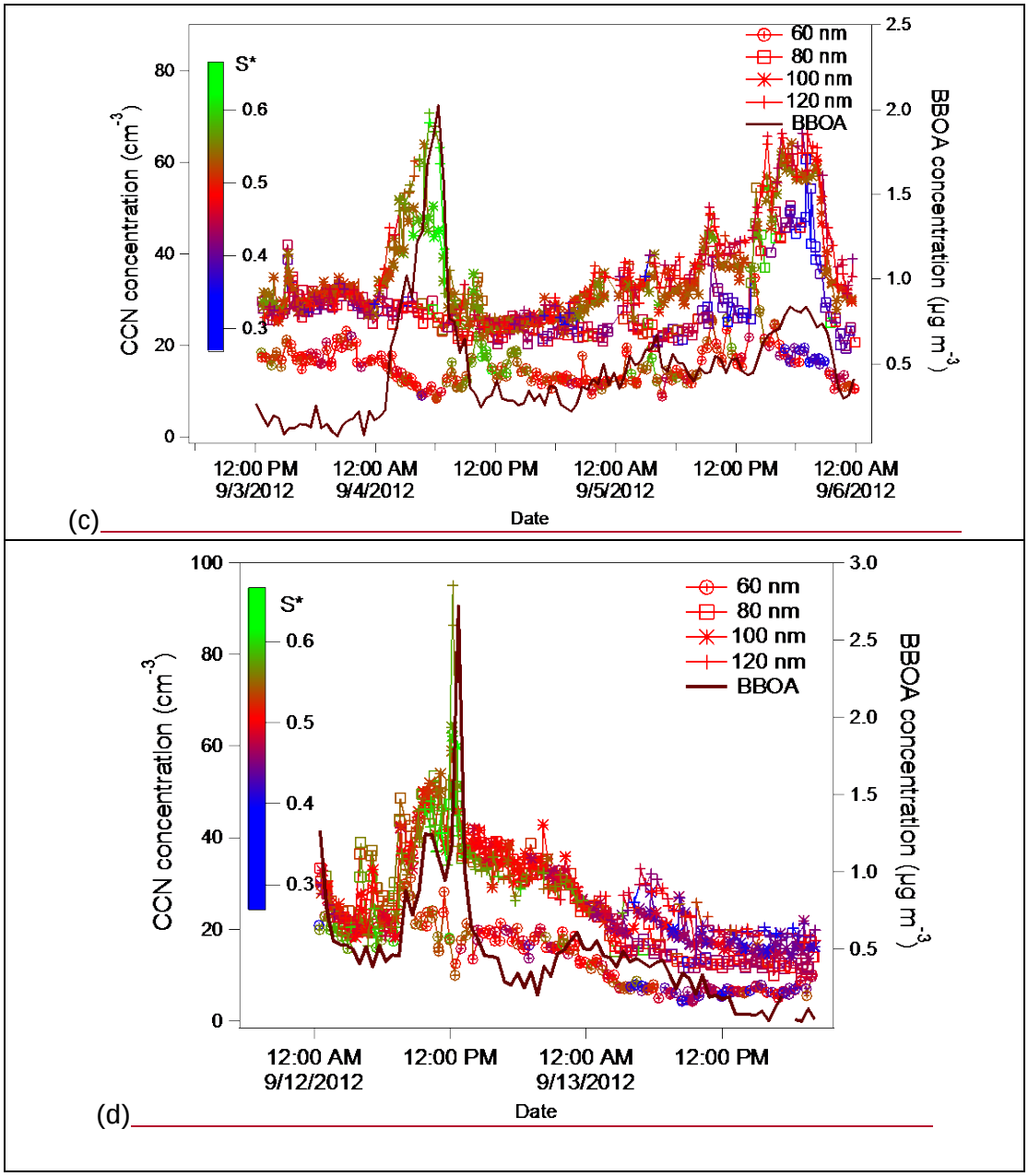
S*
0.6
0.5
0.4
0.3
60 nm
80 nm
100 nm
120 nm
BBOA
CCN concentration (cm^{-3})
BBOA concentration (μg m^{-3})
12:00 PM 9/3/2012
12:00 AM 9/4/2012
12:00 PM
12:00 AM 9/5/2012
12:00 PM
12:00 AM 9/6/2012
Date
(c)
12:00 AM 9/12/2012
12:00 PM
12:00 AM 9/13/2012
12:00 PM
Date
(d)

Figure 5

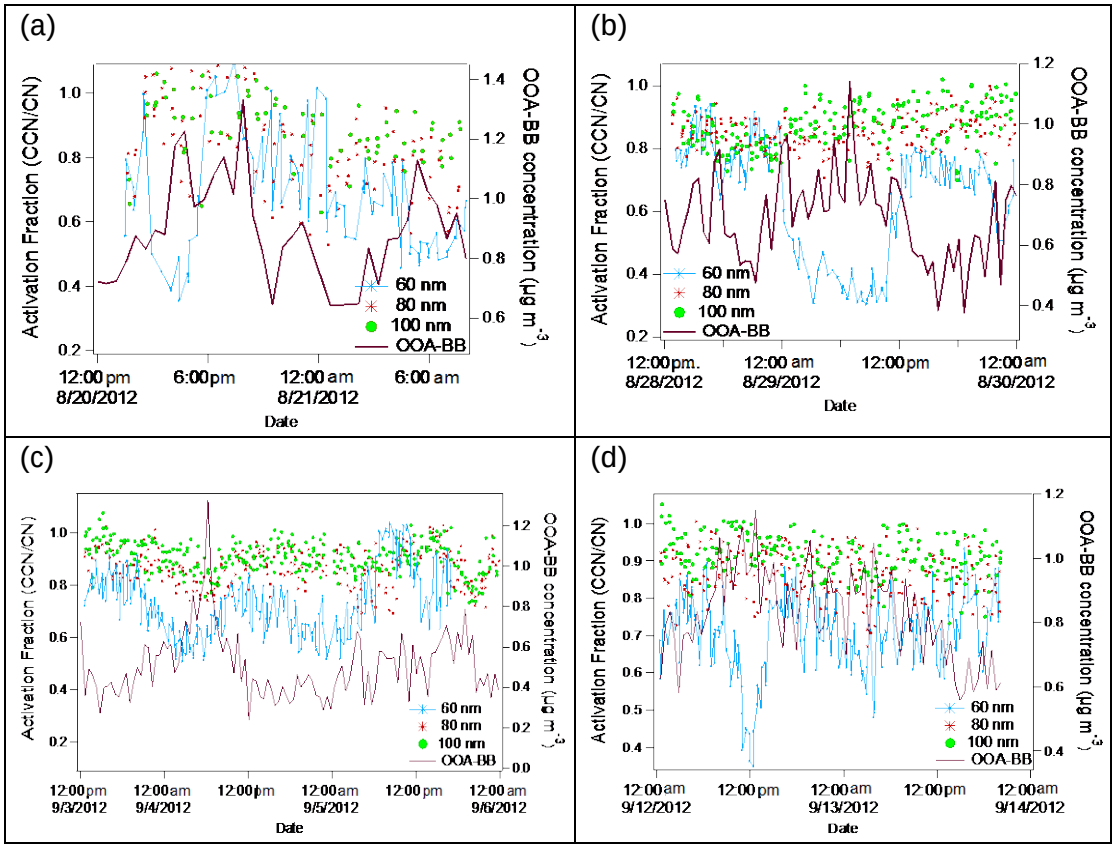
(a)
Activation Fraction (CCN/CN)
OOA-BB concentration (μg m-3)
60 nm
80 nm
100 nm
OOA-BB
12:00 pm 8/20/2012
6:00pm
12:00 am 8/21/2012
6:00 am
Date
(b)
Activation Fraction (CCN/CN)
OOA-BB concentration (μg m-3)
60 nm
80 nm
100 nm
OOA-BB
12:00pm. 8/28/2012
12:00 am 8/29/2012
12:00pm
12:00am 8/30/2012
Date
(c)
Activation Fraction (CCN/CN)
OOA-BB concentration (μg m-3)
60 nm
80 nm
100 nm
OOA-BB
12:00pm 9/3/2012
12:00am 9/4/2012
12:00pm
12:00am 9/5/2012
12:00pm
12:00am 9/6/2012
Date
(d)
Activation Fraction (CCN/CN)
OOA-BB concentration (μg m-3)
60 nm
80 nm
100 nm
OOA-BB
12:00am 9/12/2012
12:00pm
12:00am 9/13/2012
12:00pm
12:00am 9/14/2012
Date

Figure 6

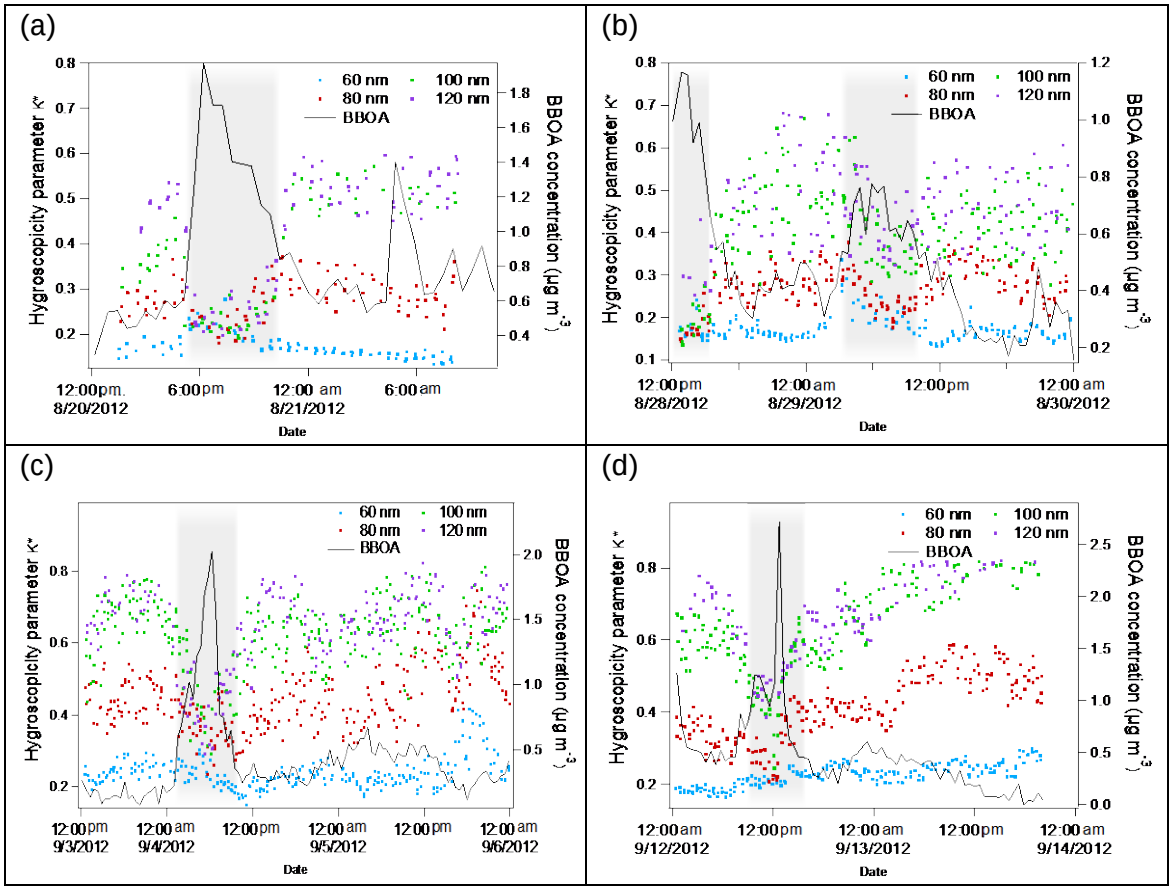
(a)
(b)
(c)
(d)
60 nm
80 nm
100 nm
120 nm
BBOA
Hygroscopicity parameter κ*
BBOA concentration (μg m-3)
Date
12:00pm. 8/20/2012
6:00pm
12:00 am 8/21/2012
6:00am
12:00pm 8/28/2012
12:00am 8/29/2012
12:00pm
12:00am 8/30/2012
12:00pm 9/3/2012
12:00am 9/4/2012
12:00pm
12:00am 9/5/2012
12:00pm
12:00am 9/6/2012
12:00am 9/12/2012
12:00pm
12:00am 9/13/2012
12:00pm
12:00am 9/14/2012

Figure 7

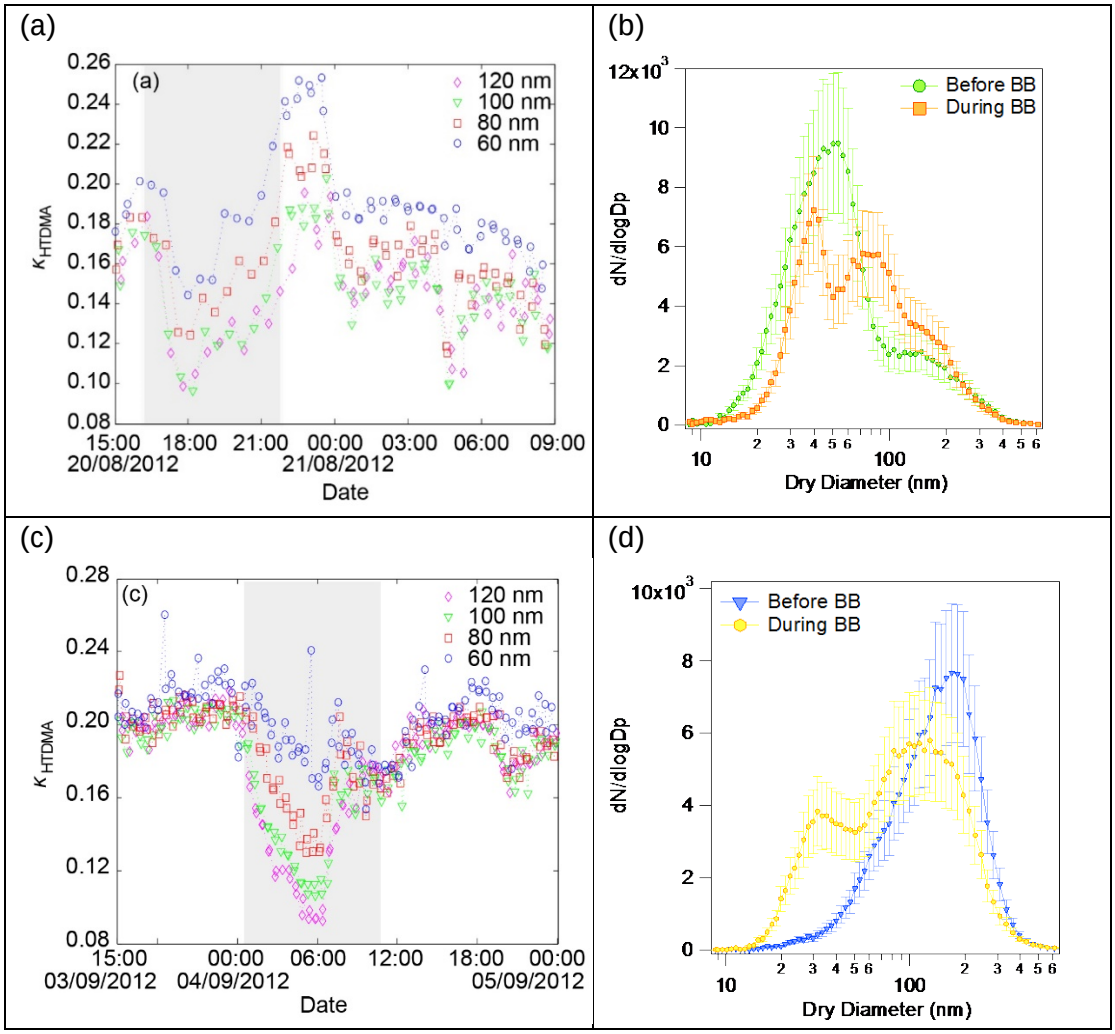
(a)
(a)
120 nm
100 nm
80 nm
60 nm
κHTDMA
0.26
0.24
0.22
0.20
0.18
0.16
0.14
0.12
0.10
0.08
15:00 18:00 21:00 00:00 03:00 06:00 09:00
20/08/2012 21/08/2012
Date
(b)
12x10^3
10
8
6
4
2
0
dN/dlogDp
Before BB
During BB
10 2 3 4 5 6 100 2 3 4 5 6
Dry Diameter (nm)
(c)
(c)
120 nm
100 nm
80 nm
60 nm
κHTDMA
0.28
0.24
0.20
0.16
0.12
0.08
15:00 00:00 06:00 12:00 18:00 00:00
03/09/2012 04/09/2012 05/09/2012
Date
(d)
10x10^3
8
6
4
2
0
dN/dlogDp
Before BB
During BB
10 2 3 4 5 6 100 2 3 4 5 6
Dry Diameter (nm)

Figure 8

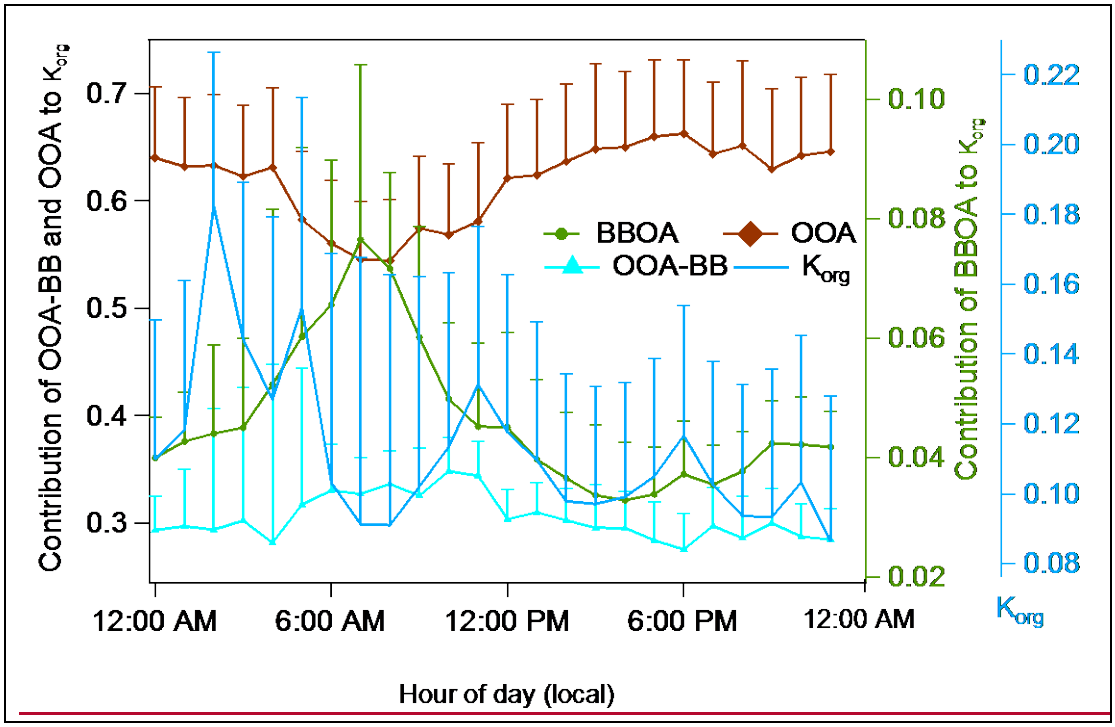
Contribution of OOA-BB and OOA to K_{org}
0.7
0.6
0.5
0.4
0.3
BBOA
OOA
OOA-BB
K_{org}
0.10
0.08
0.06
0.04
0.02
Contribution of BBOA to K_{org}
0.22
0.20
0.18
0.16
0.14
0.12
0.10
0.08
K_{org}
12:00 AM
6:00 AM
12:00 PM
6:00 PM
12:00 AM
Hour of day (local)

Figure 9

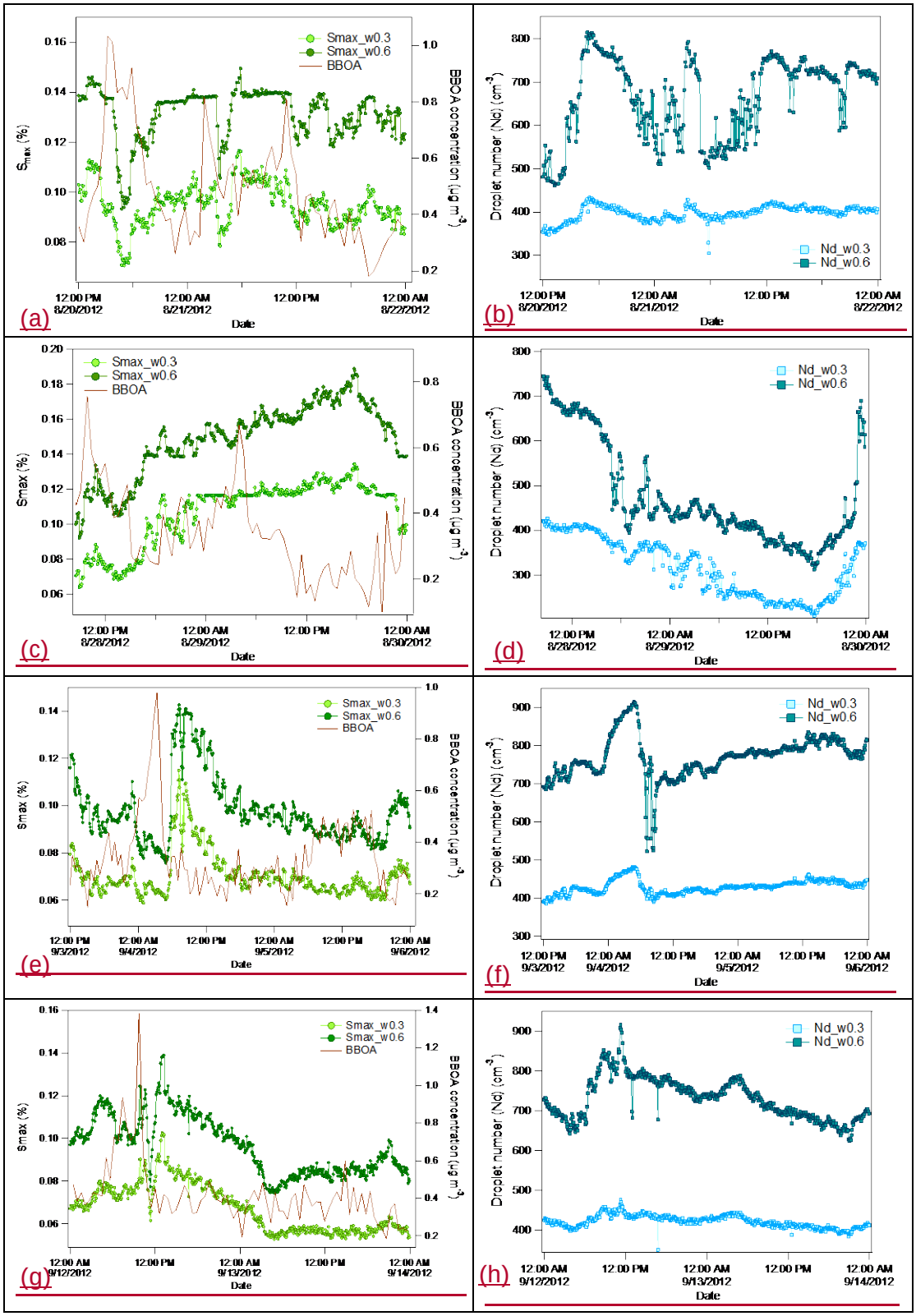
(a)
Smax_w0.3
Smax_w0.6
BBOA
Smax (%)
BBOA concentration (μg m-3)
12:00 PM 8/20/2012
12:00 AM 8/21/2012
12:00 PM
12:00 AM 8/22/2012
Date
(b)
Droplet number (Nd) (cm-3)
Nd_w0.3
Nd_w0.6
(c)
(d)
(e)
12:00 PM 9/3/2012
12:00 AM 9/4/2012
12:00 AM 9/5/2012
12:00 AM 9/6/2012
(f)
(g)
12:00 AM 9/12/2012
12:00 AM 9/13/2012
12:00 AM 9/14/2012
(h)

Figure 10

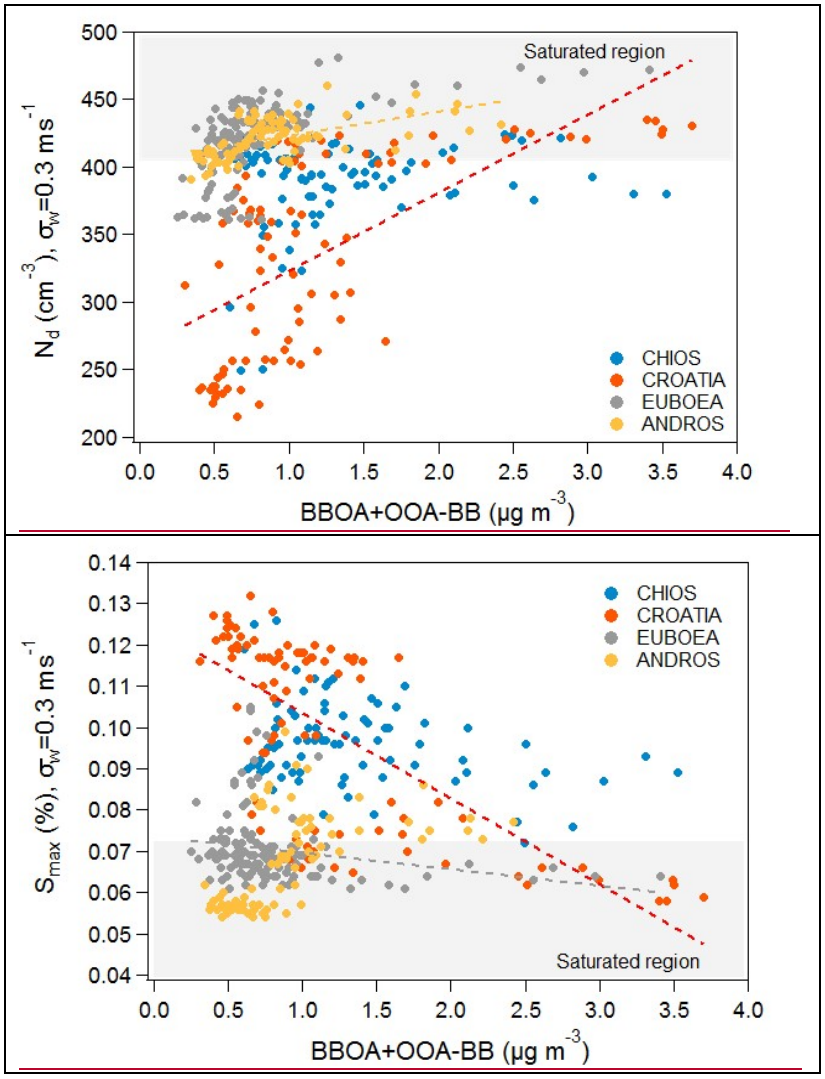
Saturated region
N_d (cm^{-3}), σ_w=0.3 ms^{-1}
BBOA+OOA-BB (μg m^{-3})
CHIOS
CROATIA
EUBOEA
ANDROS
S_{max} (%), σ_w=0.3 ms^{-1}
Saturated region
BBOA+OOA-BB (μg m^{-3})